

摘要

人类免疫缺陷病毒(HIV) DNA 疫苗能够同时诱导细胞免疫和体液免疫反应,因此为了阻止获得性免疫缺损综合征(AIDS)广泛传播,急需开发一种安全、高效的 HIV DNA 疫苗进行预防和治疗。然而,由于 DNA 抗原递送到目标抗原提呈细胞并被其摄取的几率低,抗原表达效率差,导致 DNA 疫苗免疫原性非常低。本课题组在前期研究发现两性离子脂质分子硬脂酰磷酸乙醇胺-聚羧酸甜菜碱(DSPE-PCB)具有溶酶体逃逸的能力。受此启发,我们构建了一个两性离子包覆的阳离子脂质体作为 DNA 抗原的递送载体来增加疫苗的免疫原性。同时,我们加入甘露糖作为体系的靶向分子增加抗原提呈细胞的靶向性。以此构建的阳离子脂质体体系(Man-ZCL)能够复合 DNA 抗原形成一个紧密结构来保护其免受体内核酶的降解。体外、体内实验结果表明,与 CpG/DNA 和商售试剂 Lipofectamine2000/DNA 相比,构建的靶向疫苗剂型(Man-ZCL/lipoplexes)具有显著增强的抗 HIV 免疫反应和较低的毒性,而且能够诱导 Th1/Th2 混合型免疫作用。同时,靶向疫苗剂型(Man-ZCL/lipoplexes)在免疫注射位点具有抗原储库效应,这使得 DNA 抗原能够更多地在淋巴结富集。更重要的是,靶向疫苗剂型(Man-ZCL/lipoplexes)能够通过非炎症方式辅助激活 T 细胞。这些都说明我们构建的靶向疫苗递送载体(Man-ZCL)能够作为一种安全、高效的 DNA 佐剂用于 HIV 疫苗的应用。



Enhanced non-inflammasome mediated immune responses by mannosylated zwitterionic-based cationic liposomes for HIV DNA vaccines



Chenmeng Qiao^{a, b, 1}, Jiandong Liu^{c, 1}, Jun Yang^{a, 1}, Yan Li^a, Jie Weng^{b, **},
Yiming Shao^{c, ***}, Xin Zhang^{a, *}

^a National Key Laboratory of Biochemical Engineering, Institute of Process Engineering, Chinese Academy of Sciences, Beijing 100190, PR China

^b Key Laboratory of Advanced Technologies of Materials, Ministry of Education, School of Materials Science and Engineering, Southwest Jiaotong University, Chengdu 610031, PR China

^c State Key Laboratory for Infectious Disease Prevention and Control, National Center for AIDS/STD Control and Prevention, Chinese Center for Disease Control and Prevention, Collaborative Innovation Center for Diagnosis and Treatment of Infectious Diseases, Beijing 102206, PR China

ARTICLE INFO

Article history:

Received 28 October 2015

Received in revised form

21 January 2016

Accepted 25 January 2016

Available online 29 January 2016

Keywords:

Mannosylated zwitterionic-based cationic liposome

HIV DNA vaccine

Adjuvant

Non-inflammasome pathway

Immune response

ABSTRACT

Human immunodeficiency virus (HIV) DNA vaccine can induce cellular and humoral immunity. A safe and effective HIV DNA vaccine is urgent need to prevent the spread of acquired immune deficiency syndrome (AIDS). The major drawback of DNA vaccines is the low immunogenicity, which is caused by the poor delivery to antigen presenting cells and insufficient antigen expression. Sparked by the capability of endosomal/lysosomal escape of the zwitterionic lipid distearoyl phosphoethanol-amine-polycarboxybetaine (DSPE-PCB), we attempted to develop a zwitterionic-based cationic liposome with enhanced immunogenicity of DNA vaccines. The mannosylated zwitterionic-based cationic liposome (man-ZCL) was constructed as a DNA vaccine adjuvant for HIV vaccination. Man-ZCL could complex with DNA antigens to form a tight structure and protect them from nuclei enzyme degradation. Benefited from the capability of the specific mannose receptor mediated antigen processing cells targeting and enhanced endosomal/lysosomal escape, the man-ZCL lipoplexes were supposed to promote antigen presentation and the immunogenicity of DNA vaccines. *In vitro* and *in vivo* results revealed that man-ZCL lipoplexes showed enhanced anti-HIV immune responses and lower toxicity compared with CpG/DNA and Lipo2k/DNA, and triggered a Th1/Th2 mixed immunity. An antigen-depot effect was observed in the administration site, and this resulted in enhanced retention of DNA antigens in draining lymph nodes. Most importantly, the man-ZCL could assist to activate T cells through a non-inflammasome pathway. These findings suggested that the man-ZCL could be potentially applied as a safe and efficient DNA adjuvant for HIV vaccines.

© 2016 Elsevier Ltd. All rights reserved.

1. Introduction

Human immunodeficiency virus (HIV) vaccine is a cost and effective way to prevent and control the spread of the virus infection. Traditional HIV vaccines, comprised of live, attenuated or killed

viruses, have limited for further applications due to inefficiency and potential risks (e.g. undesirable local or systemic toxicities). New generations of vaccines, such as DNA vaccines [1], have attracted much attentions, since they could induce humoral and cellular immunity to a broad spectrum of infectious diseases [2–4] and keep long-lived immunity. However, the major drawback of DNA vaccines is the significantly low immunogenicity, which is caused by poor delivery of DNA to antigen presenting cells (APCs) [5] and inefficient expression due to enzyme degradation.

A majority of synthetic delivery systems have been reported to promote the cellular uptake of DNA vaccines, improve DNA release and protect them from degradation, including inorganic nanoparticles [6–8], polymers [9,10] and liposomes [11]. Among them,

* Corresponding author.

** Corresponding author.

*** Corresponding author.

E-mail addresses: jweng@swjtu.cn (J. Weng), yshao08@gmail.com (Y. Shao), xzhang@ipe.ac.cn (X. Zhang).

¹ These authors contributed equally to this work.

cationic liposomes hold great potential in DNA vaccines delivery systems due to their excellent capability to transport DNA [12] and the ability used as adjuvants [13,14]. Cationic liposomes can condense nucleic acid *via* electrostatic attraction, improve the interaction between lipoplexes and cell membranes, elicit antigen-specific cytotoxic T lymphocyte (CTL) responses, antibody production [15]. Cationic liposomes can be taken up by APCs where they eventually disassemble, thus give chance to the plasmid for entering into the nucleus. Christopher P. Locher et al. had demonstrated that mice immunized with HIV-2 Env DNA formulated with cationic liposomes (Vaxfectin) could induce a higher end-point antibody titers and a higher level of IgG subclass (IgG2a, IgG2b, total IgG, IgA and IgM) than the group immunized with naked DNA or HIV-2 Env DNA formulated with chitosan [16]. Though, many reports have proved the advantages of cationic liposomes in delivering nucleic acid, insufficient transfection efficiency and antigen presentation still hinder the application of DNA vaccines *in vivo*.

Recently, zwitterionic lipid (distearoyl phosphoethanolamine-polycarboxy- betaine, DSPE-PCB) modified cationic liposomes were reported in our group [17]. They could protect the gene cargoes in the blood circumstances and prolong circulation time. Most importantly, the PCB modification showed enhanced cellular uptake and endosomal/lysosomal escape of small interfering RNA (siRNA), and exhibited good biocompatibility *in vitro* and *in vivo*. Herein, we hypothesized that modification of cationic liposomes with zwitterionic lipids (DSPE-PCB) should facilitate DNA vaccines cellular uptake and increase DNA release, and those could result in sufficient transcription and antigen expression, eventually enhance the immunogenicity with relatively lower cytotoxicity.

It is well known that APCs, such as macrophages and dendritic cells, express a great amount of mannose receptors on the cell surfaces [18,19]. To enhance the specificity of DNA delivery, numerous studies have explored mannosylated systems for receptor-mediated endocytosis into APCs and resulted in increased antigen presentation [20–22].

Herein, a mannosylated zwitterionic-based cationic liposome (man-ZCL) was designed as DNA vaccines delivery system to promote the immunogenicity with lower cytotoxicity. In this study, zwitterionic lipid mannosylated DSPE-PCB (mannose-DSPE-PCB), cationic lipid DOTAP and helper lipid cholesterol were constructed as the DNA adjuvant (man-ZCL) (Scheme 1): mannose-DSPE-PCB could enhance the cellular accumulation and antigen presentation of DNA; DOTAP was used to complex with DNA; cholesterol could assist stability of the cationic liposomes as a helper lipid. HIV DNA plasmid Env was chosen as a model antigen, for it had been used in human trials. The cytotoxicity and transfection efficiency of the man-ZCL/DNA vaccine systems were investigated. The capability to promote the maturation of dendritic cells and induce the secretion of cytokines were deeply investigated. Both cellular and humoral immune responses of the formulations were evaluated *in vitro* and *in vivo*. To further study the effect of man-ZCL in delivery DNA antigen *in vivo*, the antigen retention at injection sites and accumulation in lymph nodes, as well as the histological analysis were investigated.

2. Materials and methods

2.1. Materials

β -propiolactone (98%), copper bromide (98%), 2-bromo-2-methylpropionyl bromide, 2-(N, N'-dimethylamino) ethyl methacrylate (DMAEMA, 98%), 4-aminophenyl α -D-mannopyranoside (mannose) (98%) and sodium dodecyl-benzenesulfonate (SDS) were obtained from J&K Scientific Ltd (Shanghai, China). N, N, N', N''-pentamethyldiethylenetriamine (PMDETA, 99%), triethylamine (TEA, 99%), potassium carbonate, sodium chloride, 3-[4, 5-

dimethylthiazol-2-yl]-2, 5-diphenyltetrazolium bromide (MTT) and *Escherichia coli* lipopolysaccharide (LPS) were purchased from Sigma–Aldrich (St. Louis, Missouri, USA). Cholesterol (95%), 1,2-distearoyl-sn-glycero-3-phosphoethanolamine (DSPE) and (2, 3-Dioleoyloxy-propyl)-trimethylammonium (DOTAP) were purchased from Advanced Vehicle Technology Ltd., Co. (Shanghai, China). Dulbecco's Modified Eagle Medium (DMEM), Roswell Park Memorial Institute (RPMI) 1640, L-glutamine, penicillin (10,000 U/mL), streptomycin (10 mg/mL), trypsin-EDTA and fetal bovine serum (FBS) and Gene transfection kit (Lipofectamine® 2000) were purchased from Invitrogen (Carlsbad, CA, USA). Opti-MEM® I reduced serum medium was obtained from Life Technologies. Label IT® Tracker™ Intracellular Nucleic Acid Localization Kits were purchased from Mirus Bio Corporation (Madison, WI, USA). YOYO-1 (1,1'-(4,4,8,8-tetramethyl-4,8-diazaundecamethylene) bis [4-[(3-methylbenzo-1,3-oxazol-2-yl) methylidene]-1,4-dihydroquinolinium] tetraiodide) was acquired from Life Technologies as a DMSO solution and diluted to 10 μ M in phosphate-buffered saline, pH 7.4 before use. The pGL 4.51 [luc2/CMV/Neo, 6.358 kbp] vector, Glo-lysis buffer and Steady-Glo Luciferase Assay System, and CellTiter 96® AQueous One Solution Cell Proliferation Assay were purchased from Promega (Madison, WI, USA). Gel green, phosphate-buffered saline (PBS, pH = 7.4), Micro BCA protein assay kit and DNase I were purchased from Beyotime Institute of Biotechnology (Nanjing, China). Triethylamine (TEA) was bought from Alfa Aesar. LysoTracker Red was purchased from Invitrogen. E.Z.N.A.™ Endo-Free Plasmid Midi Kit was obtained from Omega Bio-tek Inc (GA, USA). The dialysis bags (MWCO 1000) were from Spectrum Laboratories Inc (NJ, USA). Granulocyte macrophage colony stimulating factor (GM-CSF) and interleukin-4 (IL-4) purchased from Peprotech (Rocky Hill, USA). All antibodies used for flow cytometry analysis were purchased from eBioscience (CA, USA), including flow cytometry cell staining buffer, Alexa Fluor 700 anti-mouse CD11c (clone N418), allophycocyanin anti-mouse CD40 (clone 1C10), phycoerythrin Cy7 (PE/Cy7) anti-mouse CD86 (clone GL-1), anti-Mouse MHC Class I (H-2Kd) PerCP-eFluor® 710, fluorescein isothiocyanate (FITC) conjugated anti-mouse/rat MHC Class II (I-E) (clone 14-4-4S). The HIV DNA plasmid (pDRVI SV1.0-Env, 6.981 kbp), the HIV-1 Env peptide, and Env protein were kindly provided by Prof. Yiming Shao (National Center for AIDS/STD Control and Prevention of China CDC). Cytosine-phosphorothioate-guanineoligodeoxynucleotide (CpG-ODN) (5'-TCC ATG ACG TTC CTG ACG TT-3') was purchased from Sangon Biotech (Shanghai, China). Paraformaldehyde and 4',6-diamidino-2-phenylindole dihydrochloride (DAPI) were obtained from Solarbio Science & Technology Co., Ltd (Beijing, China). Other reagents were acquired from Sigma–Aldrich. All the reagents were of analytical grade and used without further purification. High-purity water (Milli-Q Integral) with a conductivity of 18 M Ω cm⁻¹ was used for the preparation of all aqueous solutions.

2.2. Sample synthesis

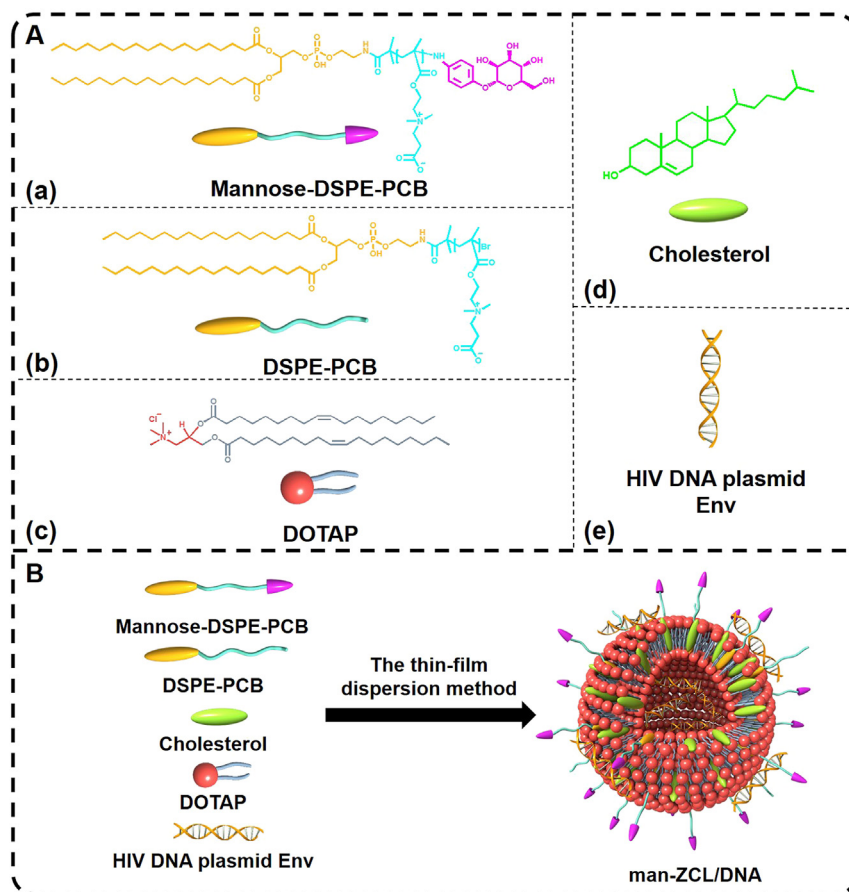
2.2.1. Synthesis of DSPE-PCB polymer

DSPE-PCB was synthesized according to the method reported by our group using an atom transfer radical polymerization (ATRP) [17]. The structure of DSPE-PCB was confirmed by ¹H NMR spectra and the degree of polymerizations of PCB was 20.

DSPE-PCB: ¹H NMR (600 MHz, CDCl₃): δ = 4.10: -OCH₂CH₂N-; δ = 3.0–4.8: -OCH₂CH₂NCH₂CH₂-; δ = 2.60: -NCH₂CH₂COO-; δ = 2.25: -NCH₃CH₃-; δ = 1.80: -NHCOCH₃; δ = 1.20–1.28: -(CH₂)₁₄-CH₃; δ = 1.00: -BrCH₂CCH₃-.

2.2.2. Synthesis of mannose-DSPE-PCB polymer

4-aminophenyl α -D-mannopyranoside (40 mg, 0.15 mmol) and potassium carbonate (16.58 mg, 0.12 mmol) were dissolved in 3 mL



Scheme 1. (A) Chemical structural formula for each components of the mannoseylated zwitterionic-based cationic lipoplexes: (a) the targeting zwitterionic lipid mannose-DSPE-PCB, (b) the zwitterionic lipid DSPE-PCB, (c) the cationic lipid DOTAP, (d) the helper lipid cholesterol and (e) the HIV DNA plasmid Env; (B) Schematic illustration of the formation of mannoseylated zwitterionic-based cationic lipoplexes (man-ZCL/DNA) by the thin-film dispersion method.

of anhydrous dimethyl sulfoxide at 85 °C with gentle stirring for 1 h. DSPE-PCB (162.42 mg, 0.03 mmol) dissolved in 3 mL of chloroform was then drop-wisely added to the aforementioned solution at 85 °C with stirring for overnight. The impurities and unreacted molecules were removed by sequentially dialyzing in a Cellu SepH1-membrane (MWCO 3500) against ethanol and deionized water for 48 h, and freeze-dried to obtain the final product.

Mannose-DSPE-PCB: $^1\text{H NMR}$ (600 MHz, CDCl_3): $\delta = 6.10\text{--}6.34$: $-\text{NHCCHCHCO}-$; $\delta = 5.73$: $-\text{OCHO}-$; $\delta = 4.10$: $-\text{OCH}_2\text{CH}_2\text{N}-$; $\delta = 3.0\text{--}4.8$: $-\text{OCH}_2\text{CH}_2\text{NCH}_2\text{CH}_2-$; $\delta = 2.60$: $-\text{NCH}_2\text{CH}_2\text{COO}-$; $\delta = 2.25$: $-\text{NCH}_3\text{CH}_3-$; $\delta = 1.80$: $-\text{BrCCH}_2\text{CH}_3$; $\delta = 1.20\text{--}1.28$: $-(\text{CH}_2)_{14}-\text{CH}_3$; $\delta = 1.00$: $-\text{BrCCH}_3-$.

2.2.3. Amplification and purification of DNA

The pGL 4.51 plasmid DNA grown in *E. coli* (JM109) cells, and was purified using E.Z.N.A.TM Endo-Free Plasmid Midi Kit according to the manufacturer's instruction. The final plasmid was re-suspended in TE buffer. 1% agarose gel electrophoresis was performed to confirm purity of the final DNA ($\text{Abs}_{260}/\text{Abs}_{280} \approx 1.88$, confirmed a high purity of DNA). The concentration of DNA was measured by UV absorption at 260 nm (Absorption Photometry) and calculated by the following Equation (1):

$$\text{DNA concentration}(\mu\text{g}/\text{mL}) = \text{Abs}_{260} \times 50 \times \text{Dilution factor} \quad (1)$$

2.3. Preparation and characterization of mannoseylated zwitterionic-based cationic liposomes (man-ZCL) and lipoplexes (man-ZCL/DNA)

2.3.1. Preparation and physicochemical characterization

The man-ZCL liposomes were prepared by a thin-film dispersion method as reported before [23]. Briefly, DOTAP, cholesterol, DSPE-PCB and mannose-DSPE-PCB ($[\text{W}_{(\text{mannose-DSPE-PCB})}]/[\text{W}_{(\text{mannose-DSPE-PCB}+\text{DSPE-PCB})}] = 20\%, 30\% \text{ and } 40\%$, respectively. W indicates the quality of the lipid) with a molar ratios of 1:1:X ($X = 0.2, 0.4, 0.6$, X refers to the total molar ratio of DSPE-PCB + mannose-DSPE-PCB in the zwitterionic-based cationic liposome) were used to construct the zwitterionic-based cationic liposomes. After dissolving in chloroform, the organic phase was removed at 55 °C on a rotary evaporator to obtain a thin lipid film, followed by incubation overnight under vacuum to remove residual solvents. The lipid films were subsequently hydrated in 8 mL of sterile PBS (pH = 7.4). After sonication at 37 °C for 30 min, the solution was extruded 5 times by using Emulsiflex-C5 high-pressure homogenizer (Avestin, Canada). These three series were marked as man-ZCL0.2, man-ZCL0.4 and man-ZCL0.6, respectively. Each series contains 20%, 30% and 40%man-ZCL (the percentage here represent the ratio of $[\text{W}_{(\text{mannose-DSPE-PCB})}]/[\text{W}_{(\text{mannose-DSPE-PCB}+\text{DSPE-PCB})}]$), respectively. Lipoplexes were prepared by mixing cationic liposomes and DNA at designed N/P ratios for 30 min at room temperature (N/P = 0.5, 1, 2, 3, 5, 8, 10 and 15, respectively).

The diameters of lipoplexes were determined by a dynamic light

scattering (DLS) instrument, and the surface zeta potentials were analyzed by the zeta potentials using a Zetasizer Nano ZS instrument (Malvern Instruments).

These lipoplexes were dripped onto 300 mesh copper grids coated with carbon and then prepared specimen by the immersion or plunging cryofixation method. To observe the morphology of man-ZCL and man-ZCL/DNA lipoplexes, cryogenic transmission electron microscopy was used (Cryo-TEM, FEI Tecnai 20, Netherlands).

2.3.2. Agarose gel electrophoresis assay

The DNA binding ability of liposomes was evaluated by agarose gel retardation assay. Lipoplexes were prepared with various N/P ratios, and naked DNA was used as a control. 20 μ L of lipoplexes were mixed with 4 μ L of 6 \times loading buffer, and then the mixture was loaded onto 1% (w/v) agarose gel containing GelGreen™ nucleic acid stain. Electrophoresis was executed out at a constant voltage of 110 V for 30 min in 1 \times TAE running buffer. The migration of DNA bands were visualized and photographed with a UV Transilluminator at a wavelength of 254 nm.

To protect the condensed DNA from nuclease degradation, the DNase I protection assay was carried [24]. The man-ZCL/DNA lipoplexes at various N/P ratios were incubated with DNase I (1 unit per 1 μ g DNA) enzyme in 10 \times reaction buffer at 37 $^{\circ}$ C for 15 min. The naked DNA treated with DNase I served as a positive control. After incubation, 1 μ L of 0.5 M EDTA was added into each sample to inactivate DNase I.

The dissociation assay was also evaluated to further confirm the binding ability of the liposomes, 5 μ L of 20 mg/mL heparin solution was added to each sample followed by incubating at room temperature for 60 min. The replacement of DNA was analyzed by agarose gel retardation assay.

2.4. *In vitro* transfection and cytotoxicity assay

To evaluate the efficiency of man-ZCL/DNA lipoplexes, RAW264.7 cells with abundant mannose receptors on their cell surfaces were selected as a model cell for *in vitro* assay [25]. RAW264.7 cells from Chinese academy of medical sciences were seeded in 24-well culture plates at 5 \times 10⁴ cells/well, and cultured in DMEM supplemented with 10% FBS, 2 mM L-glutamate, 100 U/ml penicillin and 100 μ g/mL streptomycin for 24 h before transfection. Then the medium was removed and incubated with lipoplexes containing 1 μ g of report DNA, pGL 4.51 plasmid, which has the similar length to Env. Fresh opti-MEM with different formulations were added to the wells at a pGL 4.51 plasmid dose of 1 μ g DNA per well (those formulations include PBS, naked DNA, Lipofectamine 2000/DNA and various lipoplexes with N/P = 0.5, 1, 2, 3, 5, 8, 10 and 15, respectively). RAW264.7 cells were incubated with these formulations for 4 h at 37 $^{\circ}$ C, followed by the medium was replaced with fresh medium. The cells were cultured for another 48 h and then washed with sterile PBS and lysed using the Glo Lysis Buffer, staying for 5–10 min and gently scraping off the plate. Total protein content in the cell lysates was determined by using a Micro BCA protein assay kit. The luciferase content obtained from the luminescence readings was normalized to the total protein content. All samples were tested in triplicates. *In vitro* cytotoxicity of cationic lipoplexes was assessed by an MTT colorimetric assay in RAW264.7 cells. Cells were plated onto a 96-well culture plate at a density of 1 \times 10⁴ cells/well in 100 μ L complete growth medium and allowed to attach overnight. Then, the growth medium was removed and replaced with 100 μ L fresh culture medium containing different formulations. After 48 h incubation, 20 μ L MTT solution (5 mg/mL in PBS) was added to each well and incubated at 37 $^{\circ}$ C in 5% CO₂ for 2 h. Then the solution in the well was aspirated

gently and 150 μ L DMSO was added into each well to dissolve the formazan crystal. The absorbance was measured at 570 nm using a plate reader. The percentage of cell viability was determined by comparing cells treated with different formulations to the untreated control cells. The percent relative cell viability was calculated by the following Equation (2):

$$\text{Cell viability(\%)} = \left(\frac{\text{OD}_{\text{sample}}}{\text{OD}_{\text{control}}} \right) \times 100\% \quad (2)$$

2.5. Confocal laser scanning microscope and spinning disk confocal image

The intracellular location of DNA vaccines was investigated using confocal laser scanning microscope (CLSM). Briefly, 1 \times 10⁵ RAW264.7 cells were plated into Petri dishes and allowed to attach overnight. Then, the growth medium was removed and replaced with 500 μ L fresh culture medium containing different formulations (those formulations include PBS, naked DNA, Lipofectamine 2000/DNA and various lipoplexes with N/P ratios ranging from 0.5 to 15, respectively). The HIV DNA plasmid Env was labeled with YOYO-1 (The YOYO-1 was added at the ratio of 10 μ mol YOYO-1 per 1 μ g DNA, staying at 4 $^{\circ}$ C for 1 h), and the equivalent concentration of DNA was 1 nmol. After 4 h incubation at 37 $^{\circ}$ C in 5% CO₂, the cells were washed three times with 1 \times PBS followed by staining with LysoTracker Red for 20 min at 37 $^{\circ}$ C. And then the cells were washed three times with 1 \times PBS and fixed in 4% paraformaldehyde for 10 min at room temperature. Finally, the nuclei was stained with DAPI for 10 min at room temperature. The fluorescence was observed using a Zeiss LSM780 confocal microscopy.

The endosomal/lysosomal co-localization and escape of different formulations with YOYO-1 labeled DNA in real-time were taken by spinning disk confocal microscopy. In brief, 1 \times 10⁵ RAW264.7 cells were seeded into Petri dishes for 24 h. Then the cells were stained with LysoTracker Red. After 20 min incubation, cells were washed three times by 1 \times PBS. Fresh DMEM medium containing CpG/DNA or man-ZCL0.4/5 formulations (with 1 nmol YOYO-1 labeled DNA) was added. The cells were observed by using UltraVIEW VoX spinning disk confocal microscopy (PerkinElmer, England) for 3.5 h.

2.6. Culture and stimulation of bone marrow-derived dendritic cells

2.6.1. Bone marrow-derived dendritic cells (BMDCs)

Primary murine bone-marrow-derived DC (BMDC) cultures were generated from BALB/c mice as described previously [26]. Female BALB/c mice were purchased from the Academy of Military Medical Sciences of China. All procedures involving experimental animals were performed in accordance with protocols approved by the institutional Animal Care and Use Committee of Peking University. Following mouse euthanasia and bone excision, attached tissues and muscles were dissected away. The ends of the bone were pierced with a needle of 1 mL syringe and the marrow was flushed with 5 mL of RPMI-1640 medium supplemented with 1% (v/v) penicillin/streptomycin and 10% (v/v) fetal bovine serum. After centrifugation, the cells were re-suspended in DC medium (RPMI 1640 containing 1% L-glutamine, 1% penicillin-streptomycin solution, 10% heat inactivated fetal bovine serum (FBS) supplemented with GM-CSF (20 ng/mL) and IL-4 (20 ng/mL)). The cells were then seeded into 24-well plates in 1 mL of DC medium and incubated at 37 $^{\circ}$ C under 5% CO₂ atmosphere. On day 3, 1 mL/well fresh DC medium were added. On day 5 after plating, aggregates of immature DCs were pooled and used in subsequent experiments. The

percentage of CD11c⁺ cells in these preparations was verified using the Cytomics™ FC500 flow cytometer (Beckman Coulter, Miami, FL).

2.6.2. BMDC maturation and cytokines secretion

The expression of cell surface markers including CD11c, CD40, CD86, MHC I and MHC II was assessed after incubation with DCs. After 48 h incubation with various formulations, the cells were collected and washed with flow buffer. Then the cells were stained with Alexa Fluor 700 anti-mouse CD11c (clone N418) in combination with staining for either allophycocyanin anti-mouse CD40 (clone 1C10), phycoerythrin Cy7 (PE/Cy7) anti-mouse CD86 (clone GL-1), anti-Mouse MHC Class I (H-2Kd) PerCP-eFluor[®] 710 or fluorescein isothiocyanate (FITC) conjugated anti-mouse/rat MHC Class II (I-E) (clone 14-4-4S), respectively, for 30 min at 4 °C. After centrifugation at 1000 rpm for 3 min, the supernatant was discarded and the cell suspension was obtained by adding cell staining buffer.

The cytokines secretion was assayed in DCs after the 48 h incubation with various formulations by enzyme-linked immunosorbent assay (ELISA). The absorbance at 450 nm (with 620 nm as reference) was measured by an Infinite M200 Microplate Spectrophotometer (Tecan, Männedorf, Switzerland).

2.6.3. BMDC proliferation

Immature BMDCs were seeded in 96-well culture plates in RPMI-1640 complete mediums and then stimulated for 48 h at 37 °C with PBS, 1 µg naked DNA, LPS (1 µg/mL) or man-ZCL/DNA lipoplexes with N/P ratio ranged from 3 to 5. Numbers of living cells were quantified using the CellTiter 96[®] AQueous One Solution Cell Proliferation Assay kit following the manufacturer instructions. Absorbance was measured at 490 nm using the Varioskan[®] Flash plate reader (Thermo Scientific, Pittsburgh, PA, USA). Relative cell proliferation was calculated using by the following Formula (3):

$$\text{Cell Proliferation}(\%) = \frac{A_{\text{sample}} - A_{\text{blank}}}{A_{\text{control}} - A_{\text{blank}}} \times 100\% \quad (3)$$

2.7. Immunization strategy and HIV-specific immune responses in vivo

Female BALB/c mice (6–8 weeks of age, 20–25 g of body weight) were purchased from Laboratory Animal Center of the Academy of Military Medical Sciences of China. All procedures involving experimental animals were approved by the China CDC Animal Care and Use Committee. The mice were randomly divided into eight groups and each group contains 6 mice. The mice were immunized with different formulations at week 0 and 3. The dose of DNA vaccine was 50 µg per mouse for each immunization. Vaccine formulations were administered intramuscularly (i.m.) and divided equally between two hind quadriceps muscles. 100 µL saline with 50 µg naked DNA (HIV DNA plasmid Env) was used as a negative control. 100 µL CpG/DNA (50 µg CpG+50 µg HIV DNA plasmid Env) was used as a positive control. Serum was collected by retro-orbital puncture at week 0, 3 and 6 for the antibody detection and all mice were sacrificed 3 weeks after the last immunization for immunological assays.

Antigen-specific cellular immune responses were evaluated by intracellular cytokine staining (ICS) assay according to a previous report [27]. Briefly, splenocytes were harvested from immunized mice and red blood cells were lysed using ACK buffer. Splenocytes were then stimulated with 1 µg/mL of clade-matched peptide (Env peptide) pools for 4 h, and then incubated at 4 °C for overnight. Each

condition, with the exception of the negative controls, was then stained with cell surface antibodies: anti-CD3 PerCP, anti-CD44 PE, anti-CD8 Pacific Blue (BD Pharmingen, San Diego, CA), and LIVE/DEAD[®] Fixable Blue Dead Cell Stain kit (Invitrogen, Eugene, OR). Samples were then washed, permeabilized and fixed with Cytofix/Cytoperm (BD Biosciences, San Jose, CA), then stained with anti-TNF-α-FITC and anti-IFN-γ-APC (BD Pharmingen). The cytokine flow cytometry (CFC) protocol from BD was chosen for further optimization and validation since extensive documented standardization of this assay already exists. All samples were acquired on a FACS Calibur flow cytometer (BD) capable of measuring 18 colors (BD), collecting 100,000–200,000 lymphocyte-gated events. Samples were collected from 96-well plates using High Throughput Sample (HTS, BD) device for analysis by the LSRII. All FACS analyses were performed using FlowJo[®] software (Treestar, Inc; OR).

2.8. DNA vaccines retention at the injection sites and accumulation in lymph nodes

To detect DNA vaccines retention at injection sites, HIV DNA plasmid Env was labeled with Label IT[®] Tracker™ Intracellular Nucleic Acid Localization Kits (Madison, WI, USA). BALB/c mice were intramuscularly injected in the hind quadriceps muscles with different vaccine formulations containing DNA labeled with the near-infrared dye Cy5 (25 µg HIV DNA plasmid Env per mouse). The fluorescence was recorded by Care stream FX PRO *in vivo* imaging system at the indicated time points (excitation: 649 nm; emission: 670 nm). Care stream Molecular Imaging Software was used to quantify relative fluorescence intensity at the injection sites.

To investigate the accumulation of DNA in lymph nodes, popliteal lymph node and spleen were removed at 48 h after injection with different DNA vaccine formulations. The fluorescence in spleen and popliteal lymph node was documented by the same system as aforementioned.

2.9. Hematoxylin-eosin (H&E) staining

Vaccine-associated inflammation at injection sites was analyzed by histological analysis. Female BALB/c mice (n = 3) were administered intramuscularly (i.m.) with an equivalent amount of 50 µg DNA. Vaccine formulations divided equally between two hind quadriceps muscles. 100 µL saline with 50 µg naked DNA was used as a negative control. 100 µL CpG/DNA (50 µg CpG+50 µg HIV DNA plasmid Env) was used as a positive control. After 48 h post injection, muscles at injection sites isolated from each mouse were collected, fixed and processed for H&E staining. Histological micrographs of muscle tissue sections were obtained using a Nikon light microscope with 200× magnification. From the H&E images, the inflammatory responses (the color features, purple blue/red) and cell morphology (cytoskeleton, necrosis) were evaluated.

2.10. Statistical analysis

All data were presented as mean ± standard deviation (SD). Presented data were representative for at least 3 independent experiments. The differences/correlations between two groups were analyzed by using Student's t-test, and the differences between the control group and the experimental groups were analyzed by using one-factor analysis of variance (ANOVA). Data were considered statistically to be significant at P < 0.05.

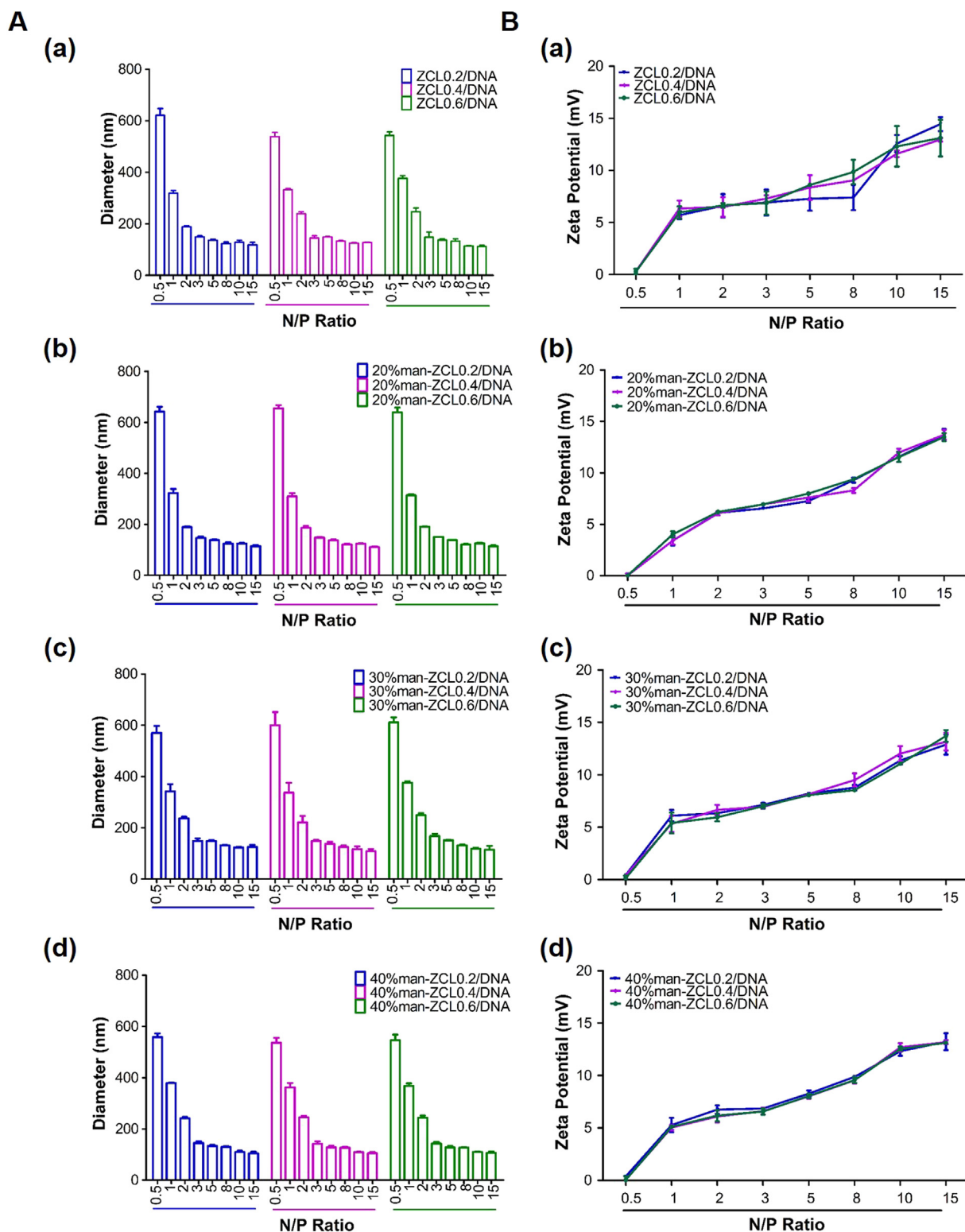


Fig. 1. DLS characterization of ZCL/DNA, 20%, 30% and 40%man-ZCL/DNA lipoplexes. (A) Diameters and (B) zeta potentials of (a) ZCL/DNA lipoplexes, (b) 20%man-ZCL/DNA lipoplexes, (c) 30% man-ZCL/DNA lipoplexes and (d) 40%man-ZCL/DNA lipoplexes at various N/P ratios.

3. Results and discussions

3.1. Preparation and characterization of mannose-modified zwitterionic polymer (mannose-DSPE-PCB)

DSPE-PCB was prepared by the ATRP of DSPE-based initiator

(DSPE-Br) and CB with CuBr/PMDETA as the catalyst. The structure of DSPE-PCB was confirmed by ^1H NMR spectrum (Fig. S1A). Calculated from the spectrum, the degree of polymerizations (DPs) of PCB, which was calculated by the area of characteristic peaks of DSPE-Br ($\delta = 1.20\text{--}1.28$ ppm: $-(\text{CH}_2)_{14}-\text{CH}_3$) and CB monomer ($\delta = 4.58$ ppm: $-\text{OCH}_2\text{CH}_2\text{N}-$), was 20. The mannose-DSPE-PCB was

synthesized by conjugating targeting molecules mannose with DSPE-PCB by using K_2CO_3 as the acid scavenger. Untreated mannose was removed by sequentially dialyzing with ethanol and distilled water. The conjugation was confirmed by the 1H NMR spectrum (Fig. S1B), which displayed the characteristic peak of mannose ($\delta = 6.05\text{--}6.31$: $-\text{CCHCHCCHCH}-$).

3.2. Diameter, zeta potential and morphology of the zwitterionic-based cationic liposomes (ZCL) and lipoplexes (ZCL/DNA)

As shown in Table S1, the diameter of the bare liposome was around 100 nm, and the zeta potential was range from 14 to 16 mV. After complex with DNA, the diameters of lipoplexes at N/P 0.5 were all more than 500 nm, and the charges were electrically neutral (Fig. 1A, B). This indicated that these liposomes were not sufficient to complex with DNA at this ratio, and the lipoplexes preferred to aggregate to form stable structure. The large state of aggregation made them inappropriate as gene delivery vectors for *in vivo* applications [28]. The diameters of the lipoplexes decreased with the N/P ratio increased to 2. And the diameter tended to a platform when the N/P ratios were larger than 3. This demonstrated that DNA could be effectively complex with ZCL to form a compact lipoplex when N/P ratio larger than 3 (0 S2). The zeta potential of lipoplexes increased as the N/P ratio increased (Fig. 1B, a–d). For instance, the zeta potential of 30%man-ZCL0.4/DNA lipoplexes was increased from 0.32 mV at N/P 0.5–12.94 mV at N/P 15 (Fig. 1B, c). This demonstrated that the zeta potential of ZCL lipoplexes increased along with the complexation of ZCL or man-ZCL. The diameter and zeta potential of man-ZCL and their corresponding lipoplexes exhibited the similar tendency and had no significant difference with ZCL. Also, the spherical shape of zwitterionic-based cationic lipoplexes was confirmed by Cryo-TEM images (Fig. 2, A–E). These results reflected the fact that the zwitterionic-based cationic liposomes had a strong ability to condense with DNA, which was a crucial factor in liposomal vaccine design [29].

3.3. DNA condensation and stability of lipoplexes

Efficient condensation of DNA into stable lipoplexes *via* electrostatic interactions is of great importance to protect the DNA from nuclease degradation as well as facilitate its cellular uptake [30]. Agarose gel retardation assay was performed to evaluate the DNA condensation capability of man-ZCL. As shown in Fig. 3A, the complete retardation of DNA was achieved at N/P ratio range from 0.5 to 15 for all four series of formulations, suggesting that man-ZCL could complex with DNA at the tested N/P range.

Numerous enzymes presented in the organism were a great challenge for the effective transcription of DNA released from lipoplexes. Effective protection of DNA from degradation by DNase was an essential prerequisite for man-ZCL. Hence, the man-ZCL/DNA lipoplexes were incubated with DNase I enzyme for

15 min at 37 °C and then explored *via* the gel electrophoresis. Man-ZCL/DNA lipoplexes could efficiently protect the bounded DNA from DNase I degradation at the tested N/P ratios (Fig. 3B) without conformation changes (Fig. S3). This demonstrated that man-ZCL could provide enough protection for DNA vaccines for *in vitro* and *in vivo* applications, and achieve much more cellular accumulation for antigen presentation.

For further investigating the stability of man-ZCL/DNA lipoplexes, competition assay for heparin (the heparin/DNA weight ratio was 50/1) was executed. The heparin was used to dissociate the lipoplexes due to its strong electrostatic competitive interaction with cationic liposomes. Seen from Fig. 3C, generally speaking, the DNA could not be replace by heparin when N/P ratio was larger than 5. For example, the complete retardation was appeared when the N/P ratios were more than 3, 2 and 1 for 30%man-ZCL0.2/DNA, ZCL0.4/DNA and ZCL0.6/DNA lipoplexes, respectively. The data revealed that the constructed liposomes provided enough protection against various challenges, including DNase degradation and heparin replacement.

3.4. *In vitro* cytotoxicity and transfection ability

The favorable biocompatibility and efficient DNA transfection is a challenge for DNA adjuvant design [31]. To evaluate the biocompatibility of the zwitterionic-based cationic liposomes, the cytotoxicity of the corresponding lipoplexes was estimated by MTT assay against RAW264.7 cells, which were used as a model of APCs with abundant of mannose receptors on their cell surfaces [25]. Naked DNA and commercial transfection reagent Lipofectamine[®] 2000 complexed with DNA (Lipo2k/DNA) were used as negative and positive control, respectively. As shown in Fig. 4A: (1) naked DNA had no effect on cell viability; (2) the lipo2k/DNA group presented relatively high cytotoxicity, with only 53% cell viability; (3) It was worth noting that the cell viability of three formulations groups (with 20%, 30% and 40% mannosylated systems) had the similar tendency as the ZCL group. Over all, the cytotoxicity enhanced as the N/P ratios increased, which was due to large proportion of cationic lipids in the lipoplexes (Fig. 4A, a–d). Specifically, when the N/P ratios were more than 8, there was no chance for the lipoplexes using as DNA delivery system for the severe cytotoxicity. However, when the N/P ratios were less than 5, the cell viabilities were generally more than 80%. This indicated man-ZCL/DNA lipoplexes had no significant cytotoxicity against RAW264.7 cells at N/P ratio less than 5, demonstrating a good biocompatibility of the delivery systems.

To evaluate the transfection efficiency of man-ZCL, RAW264.7 cells and pGL 4.51 plasmids were used as model cells and DNA respectively (The formed lipoplexes, which were comprised of liposomes and pGL 4.51 plasmids, showed similar physicochemical properties compared with the lipoplexes comprised of Env, including size, zeta potentials and DNA binding

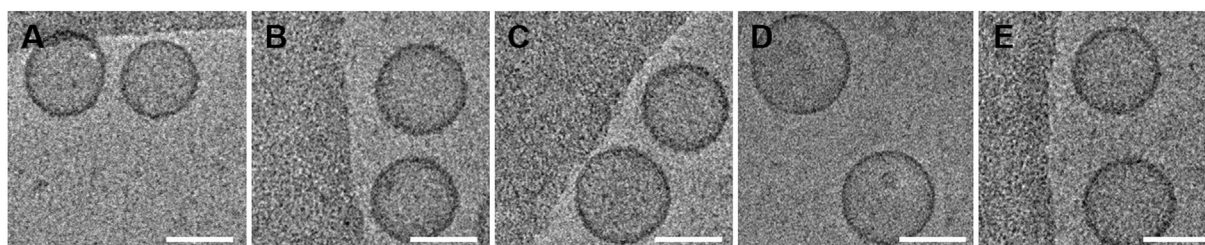


Fig. 2. The Cryo-TEM image of (A) bare liposome (ZCL0.4/DNA at N/P ratio of 5), (B) man-ZCL0.2/DNA at N/P ratio of 3, (C) man-ZCL0.4/DNA at N/P ratio of 3, (D) man-ZCL0.4/DNA at N/P ratio of 5 and (E) man-ZCL0.6/DNA at N/P ratio of 3 lipoplexes. (The concentration of mannose was 30%) (Scale bar: 100 nm).

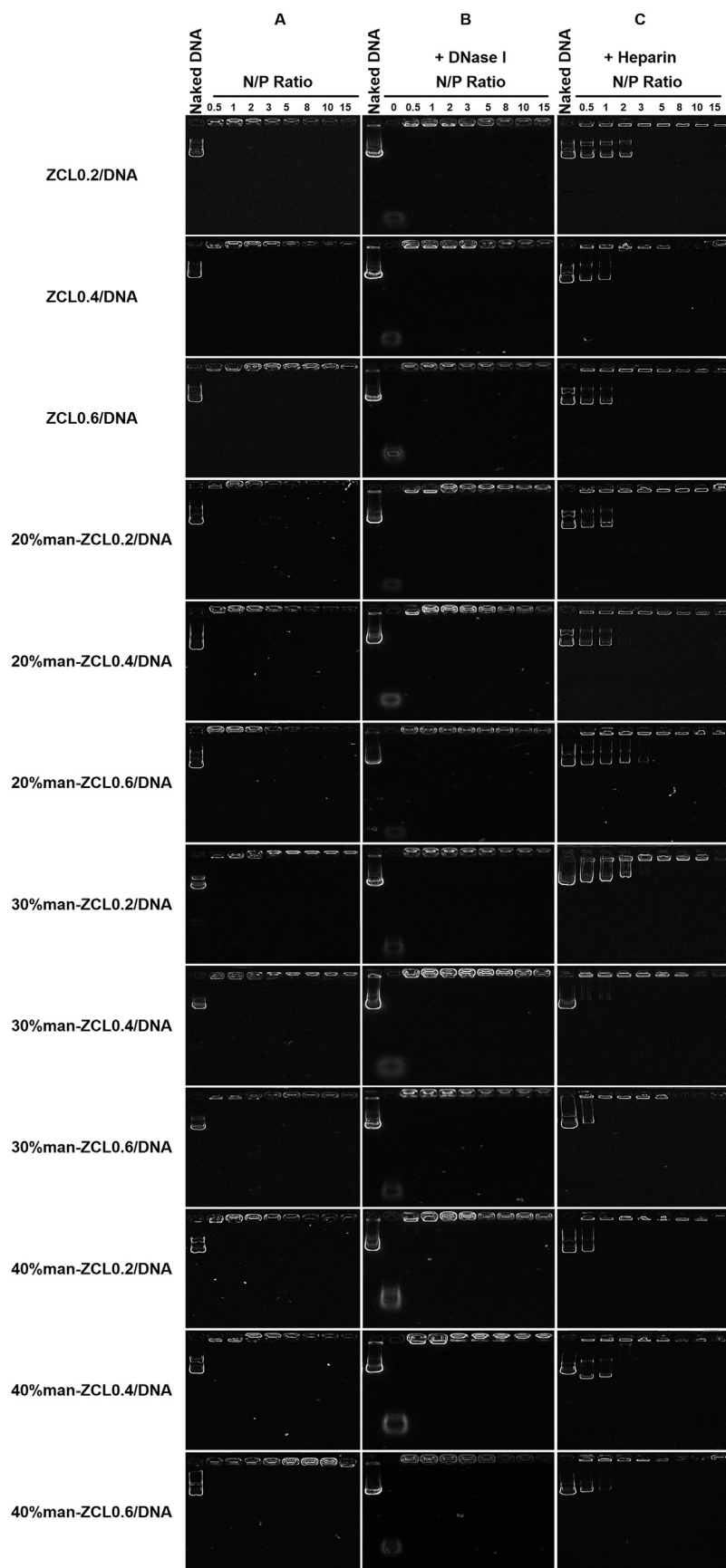


Fig. 3. Agarose gel retardation assay of zwitterionic cationic lipoplexes. (A) The DNA complexation capability of ZCL/DNA and man-ZCL/DNA lipoplexes at various N/P ratios determined by gel retardation assay. The stability of ZCL/DNA lipoplexes various N/P ratios determined by gel retardation assay; (B) The DNA protection capability of ZCL/DNA and man-ZCL/DNA lipoplexes at various N/P ratios against DNase I degradation; (C) The DNA replacement of ZCL/DNA and man-ZCL/DNA lipoplexes at various N/P ratios against heparin dissociation.

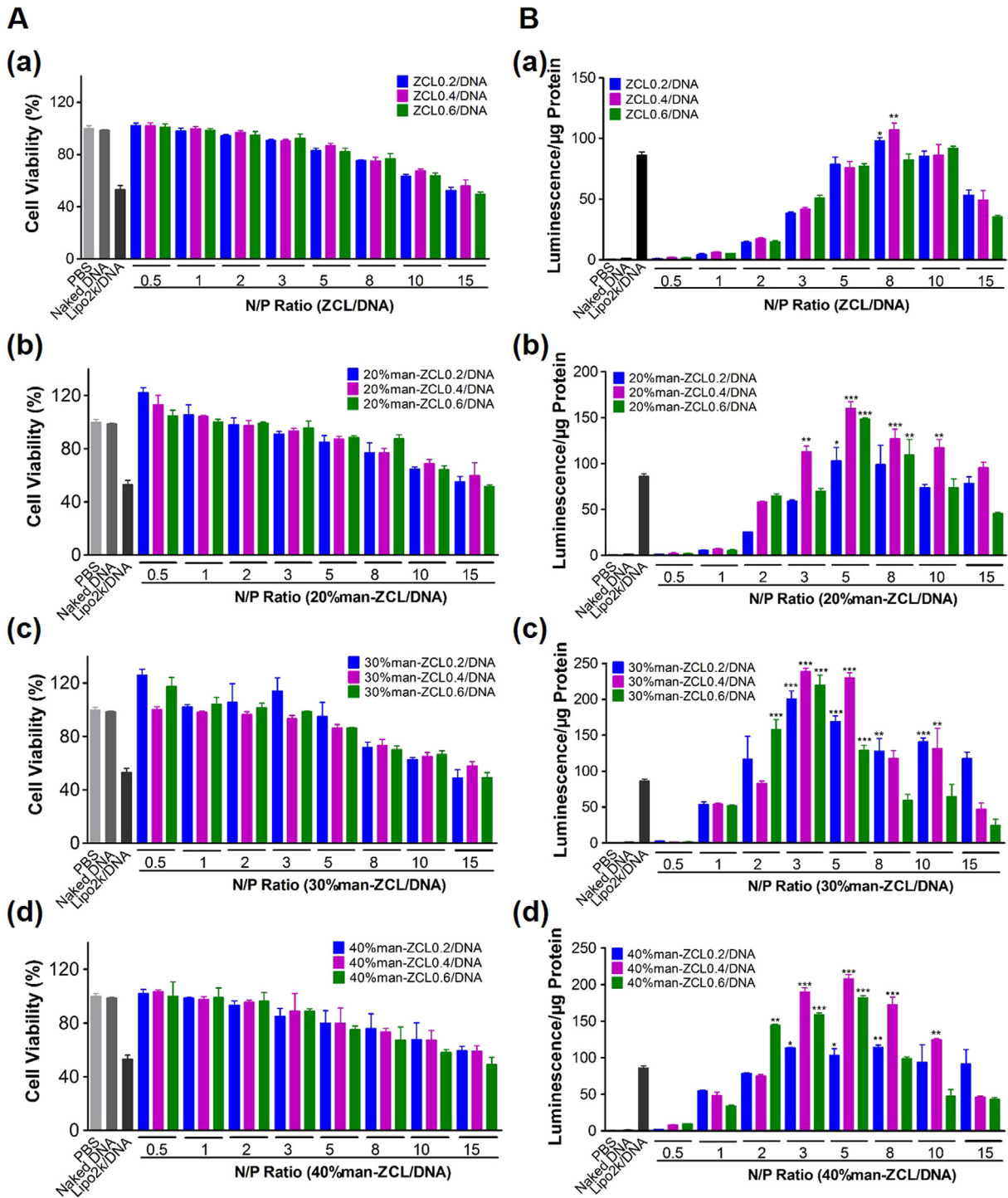


Fig. 4. *In vitro* cytotoxicity (A) and transfection efficiency (B) of ZCL/DNA and man-ZCL/DNA lipoplexes in RAW264.7 cells after 48 h of transfection. (Left: a-d) The cytotoxicity of RAW264.7 cells incubated with ZCL/DNA, 20%man-ZCL/DNA, 30%man-ZCL/DNA and 40%man-ZCL/DNA lipoplexes at N/P ratios ranging from 0.5 to 15 for 48 h, the pGL 4.51 plasmid DNA was used as a model DNA, (Right: a-d) The transfection efficiency of ZCL/DNA, 20%man-ZCL/DNA, 30%man-ZCL/DNA and 40%man-ZCL/DNA lipoplexes at N/P ratios ranging from 0.5 to 15 after 4 h transfection followed by another 48 h incubation. *: differences between Lipo2k/DNA group and man-ZCL/DNA group, *: P < 0.05, **: P < 0.01, ***: P < 0.005.

abilities (Fig. S4 and Fig. S5). As shown in Fig. 4B, man-ZCL/DNA lipoplexes exhibited better transfection efficiency compared with ZCL/DNA lipoplexes, which was due to the active targeting of the mannose and the better DNA condensation and stability of lipoplexes (Fig. 3C, take ZCL0.4 and 30%man-ZCL0.4 as examples). Besides, the transfection efficiency of ZCL/DNA lipoplexes exhibited a similar tendency with all three series of man-ZCL/DNA lipoplexes.

For example, when the N/P ratio was less than 3, the transfection efficiency of 30%man-ZCL0.4 lipoplexes increased with the N/P ratio increased (Fig. 4B, c). Whereas the transfection efficiency of 30%man-ZCL0.4 lipoplexes reduced along with the N/P ratio increased when the N/P ratio was larger than 5. Considering those physicochemical properties, a conclusion could be obtained: the lower gene expression at N/P < 3 might be caused by insufficiently

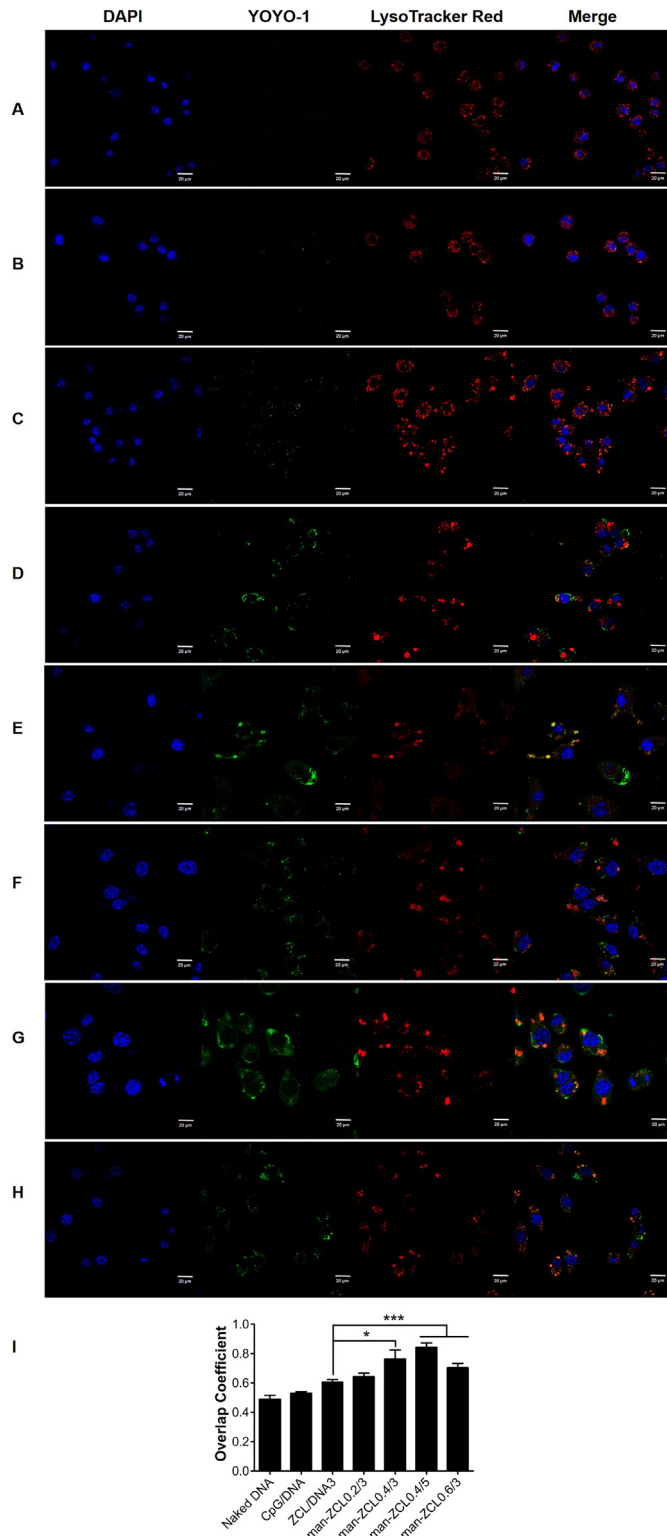


Fig. 5. The cellular uptake of YOYO-1 labeled DNA formulations assay by CLSM. CLSM images of nucleus (stained with DAPI, blue fluorescence), DNA formulations (YOYO-1 labeled DNA, green fluorescence), lysosomes (stained with LysoTracker Red, red fluorescence) and their overlay signals after incubating (A) PBS, (B) naked DNA, (C) CpG/DNA, (D) ZCL/DNA (ZCLO.4/5), (E) man-ZCLO.2/3, (F) man-ZCLO.4/3, (G) man-ZCLO.4/5, (H) man-ZCLO.6/3 formulations with RAW264.7 cells for 4 h. (I) The overlap coefficients of lysosomes and YOYO-1 Env were calculated by Zen Co-localization software. (Scale bar: 20 μ m). Data in (I) are representative for 3 results in each group. Data shown are mean \pm SD, *: differences between ZCL/DNA group with the man-ZCL/DNA groups. **: $P < 0.01$, ***: $P < 0.005$. (For interpretation of the references to color in this figure legend, the reader is referred to the web version of this article.)

binding capability of ZCL, and this was in agreement with the DNA replacement results (Fig. 3C); Instead, the main reasons for lower expression at $N/P > 8$ were the high cytotoxicity of the lipoplexes, which resulted in loss of function of RAW264.7 cells as cell death (Fig. 4A), and the inability DNA release from lipoplexes, which was caused by the high condensation of DNA at $N/P > 8$ (Fig. 3C). Taking the cytotoxicity and DNA transfection efficacy into accounts, four formulations, 30%man-ZCLO.2/3, 30%man-ZCLO.4/3, 30%man-ZCLO.6/3 and 30%man-ZCLO.4/5 (the number after '/' refers to the N/P ratio) with the higher transfection efficiency and lower cytotoxicity, were chosen for the following experiments.

3.5. Cellular uptake and endosomal/lysosomal escape of lipoplexes

The DNA in the lipoplexes needed to be internalized into the cells and escape from the endosome/lysosome efficiently to cell nuclei for protein expression and antigen presentation. Herein, the cellular uptake and intracellular distribution of the lipoplexes were assayed by confocal laser scan microscopy (CLSM) after 4 h of transfection (Fig. 5). HIV DNA plasmid Env was labeled with YOYO-1 (green fluorescence dye). Naked DNA, CpG/DNA treated group exhibited few green fluorescence (Fig. 5B, C). And a slight green fluorescence of ZCL/DNA treated group spread around the cell membranes (Fig. 5D). As shown in Fig. 5B, C, few green fluorescence was observed in groups treated with Naked DNA or CpG/DNA formulations. Although, a slight green fluorescence of ZCL/DNA treated group spread around the cell membranes (Fig. 5D), the cells incubated with man-ZCL/DNA lipoplexes displayed an obvious yellow fluorescence, the green fluorescence overlapped the red, which suggested that the lipoplexes resided in endosomes/lysosomes (Fig. 5E–H). Moreover, the cellular uptake of man-ZCL/DNA was significant higher than that of ZCL/DNA (Fig. 5I). Those results revealed that the target lipid (man-DSPE-PCB) could enhance the cellular uptake and thereby promote DNA antigen presentation, which were in agreement with the data shown in the *in vitro* transfection efficiency experiment (Fig. 4B).

To further evaluate the capability of endosomal/lysosomal escape of the man-ZCL/DNA lipoplexes, spinning disk confocal microscopy was used. Man-ZCLO.4/5 was used as a representative group and CpG/DNA as a control group. The lysosomes were labeled by LysoTracker Red and DNA by YOYO-1. As shown in Fig. 6 (A–C) and Video S1, bright yellow fluorescence was shown for 0.5 h, which mean CpG/DNA could enter into lysosomes quickly. However, small vesicles could be observed at the surface of the cell membrane, which indicated that the CpG/DNA had great toxicity to RAW264.7 cells. While the bright yellow fluorescence was shown for 1 h for the cells treated with man-ZCLO.4/5 group (Fig. 6 (D–G) and Video S2), which indicated that DNA entered into cell and co-localized with lysosomes. After incubation for 3 h, the yellow fluorescence gradually weakened and changed to dispersing green fluorescence. As we know that LysoTracker Red facilitated to accumulate in acidic organelle, especially lysosomes. When the lysosomal ruptured, the red fluorescence disappeared. Herein, this phenomenon demonstrated that DNA was escaped from endosomes/lysosome. This was in accordance with our previous report that zwitterionic liposomes could help siRNA escape from endosomes/lysosomes [17].

Supplementary data related to this article can be found online at <http://dx.doi.org/10.1016/j.biomaterials.2016.01.054>.

3.6. Bone marrow-derived dendritic cells (BMDCs) maturation, proliferation and cytokine secretion

DCs as professional antigen processing cells (APCs) played pivotal roles in stimulating both innate and adaptive immune

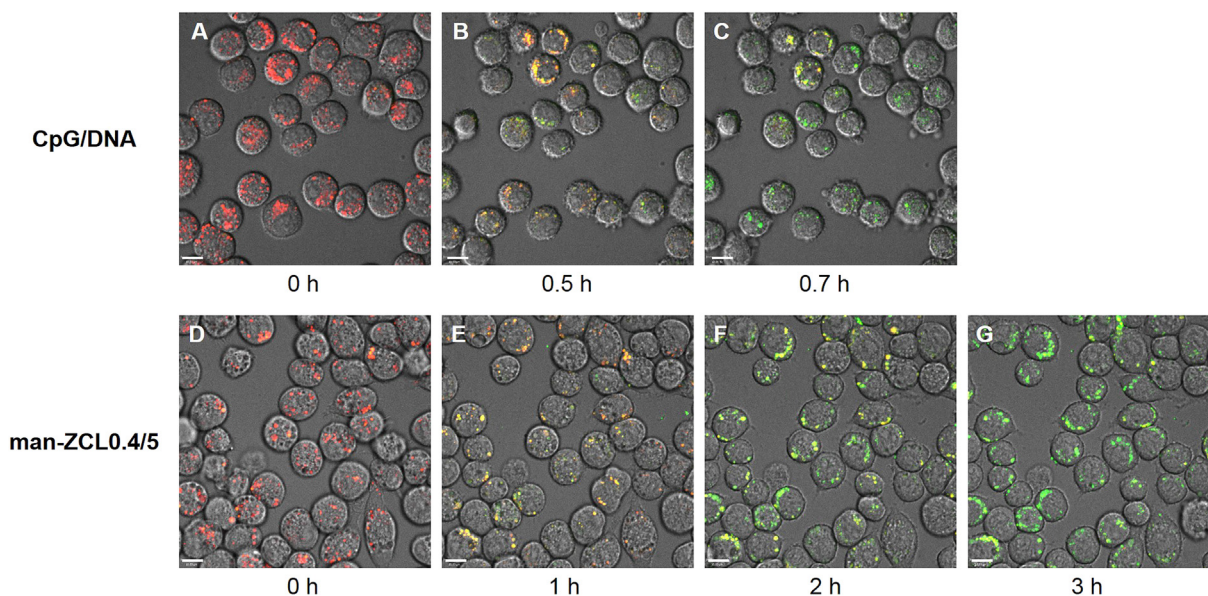


Fig. 6. Spinning disk confocal image in real-time of RAW264.7 cells following incubation with man-ZCL/DNA formulations (YOYO-1 labeled DNA) at 37 °C. The lysosomes were labeled with LysoTracker Red dye, and DNA with YOYO-1 green fluorescence dye. LysoTracker Red facilitated to accumulate in acidic organelle (lysosomes) and the fluorescence disappeared once the lysosomal ruptured. The cells were incubated with CpG/DNA for 0 h (A), 0.5 h (B) 0.7 h (C); cells treated with man-ZCL0.4/5 (YOYO-1 labeled DNA) for 0 h (D), 1 h (E), 2 h (F) and 3 h (G). (Scale bar: 10 μm). (For interpretation of the references to color in this figure legend, the reader is referred to the web version of this article.)

responses [32]. The immature DCs could take the antigen, process the antigen into peptides and present peptide-major histocompatibility complex (MHC) to naïve T cell to initiate the immune response. Herein, the degree of DC maturation, indicated by the co-stimulatory factors on the cell surfaces, was an indicator for evaluating the level of immune responses [33]. In this study, bacteria-derived lipopolysaccharide (LPS), CpG with DNA (CpG/DNA) were used as controls. As shown in Fig. 7A, the expression of CD40 and CD86 markers was enhanced for man-ZCL lipoplexes treated groups in comparison with LPS, CpG/DNA, Lipo2k/DNA and non-targeted ZCL/DNA groups. Among the man-ZCL lipoplexes, the CD40 and CD86 expression of man-ZCL0.4/5 group was significantly up-regulated, with 3.2-fold compared with naked DNA and 2.9-fold with CpG/DNA in CD40 expression (Fig. 7A, a), and 3.4-fold compared with naked DNA and 3.7-fold with CpG/DNA in CD86 expression, respectively (Fig. 7A, b). These results were coincidence with the previous observation of confocal microscopy (Fig. 5G). The man-ZCL0.4/5 presented the highest cellular uptake and protein expression, which induced enhanced maturation of DCs than other targeting formulations. This might be caused by the concentration of zwitterionic lipid DSPE-PCB in liposomes and the N/P ratio in the lipoplexes. At the same N/P ratio, possession of more DSPE-PCB could facilitate DNA antigen escaping from endosomes/lysosomes by fusion with the membranes of endosomes/lysosomes, and enhanced DNA accumulation in cell nuclei. When the concentration of DSPE-PCB increased to 0.6, the complex ability with DNA of ZCL0.6 was larger than ZCL0.4 (shown in Fig. 3C, heparin competition assay), and might limit the release of DNA from the lipoplexes. As for man-ZCL0.4/3 and man-ZCL0.4/5, the level of maturation of DC might be affected by the adjuvant of man-ZCL.

The DNA antigens taken up by antigen-processing cells eventually presented to naïve T cells, this process was associated with major histocompatibility complex class I (MHC I) and class II (MHC II) molecules. Seen from Fig. 7B, the level of MHC I of man-ZCL0.4/5 was significantly increased compared with LPS, naked DNA, Lipo2k/DNA and CpG/DNA (Fig. 7B, a); while the level of MHC II of man-ZCL lipoplexes exhibited no remarkable difference with the other groups (Fig. 7B, b). This indicated that man-ZCL0.4/5 delivery

system could promote the DNA cargoes to enter the intracellular processing pathway and stimulate the CD8⁺ T cells, and had no obvious influence on stimulation of CD4⁺ T cells. The high level of MHC I expressed on DCs for man-ZCL0.4/5 treated group suggested that man-ZCL0.4 promoted the MHC I-restricted pathway, which facilitated for cell-mediated immunity.

Meanwhile, the proliferation of DCs was also examined to evaluate the impact of lipoplexes on the capacity of DCs (Fig. 7C). After incubating with DCs for 48 h, a significant improvement of DCs proliferation was observed when treated with man-ZCL/DNA lipoplexes. And the group treated with man-ZCL0.4/5 proliferated for 5.0-fold and 8.2-fold than that of LPS and CpG/DNA groups, respectively.

The secretion of cytokines is essential in modulating inflammatory and immunological mediators. In our study, the secretion of cytokines (IL12p70, IL-6, IFN-γ and TNF-α) were evaluated by ELISA (Fig. 7D). The IL12p70 was reported to induce strong T helper type 1 (Th1) antigen-specific CD8⁺ T cell immunity. IL-6, IFN-γ and TNF-α were important inflammatory cytokines for the immune systems. Among them, TNF-α, one of the most important cytokines in the both innate and adaptive immune systems [34], is a pro-inflammatory cytokine that is not induced via the inflammasome-mediated immune response [35]. As shown in Fig. 7D (a–d), man-ZCL0.4/5 lipoplexes induced significantly higher levels of IL-12p70, IL-6, IFN-γ and TNF-α than that of naked DNA, CpG/DNA and Lipo2k/DNA. Specifically, the secretion level of TNF-α and IFN-γ were quite close to the positive control LPS group, indicating that the man-ZCL had great adjuvant effects in DNA vaccines. These data suggested that man-ZCL/DNA lipoplexes could enhance cytokines release, and induce higher levels of inflammatory cytokines, which produced through a non-inflammasome pathway. The enhancement of secretion of pro-inflammatory cytokine TNF-α via the non-inflammasome mediated immune pathway was in agreement with the previous report by Kenichi Niikura's group [34].

3.7. HIV-specific immune responses in vivo

Cellular and humoral immunity were the primary and

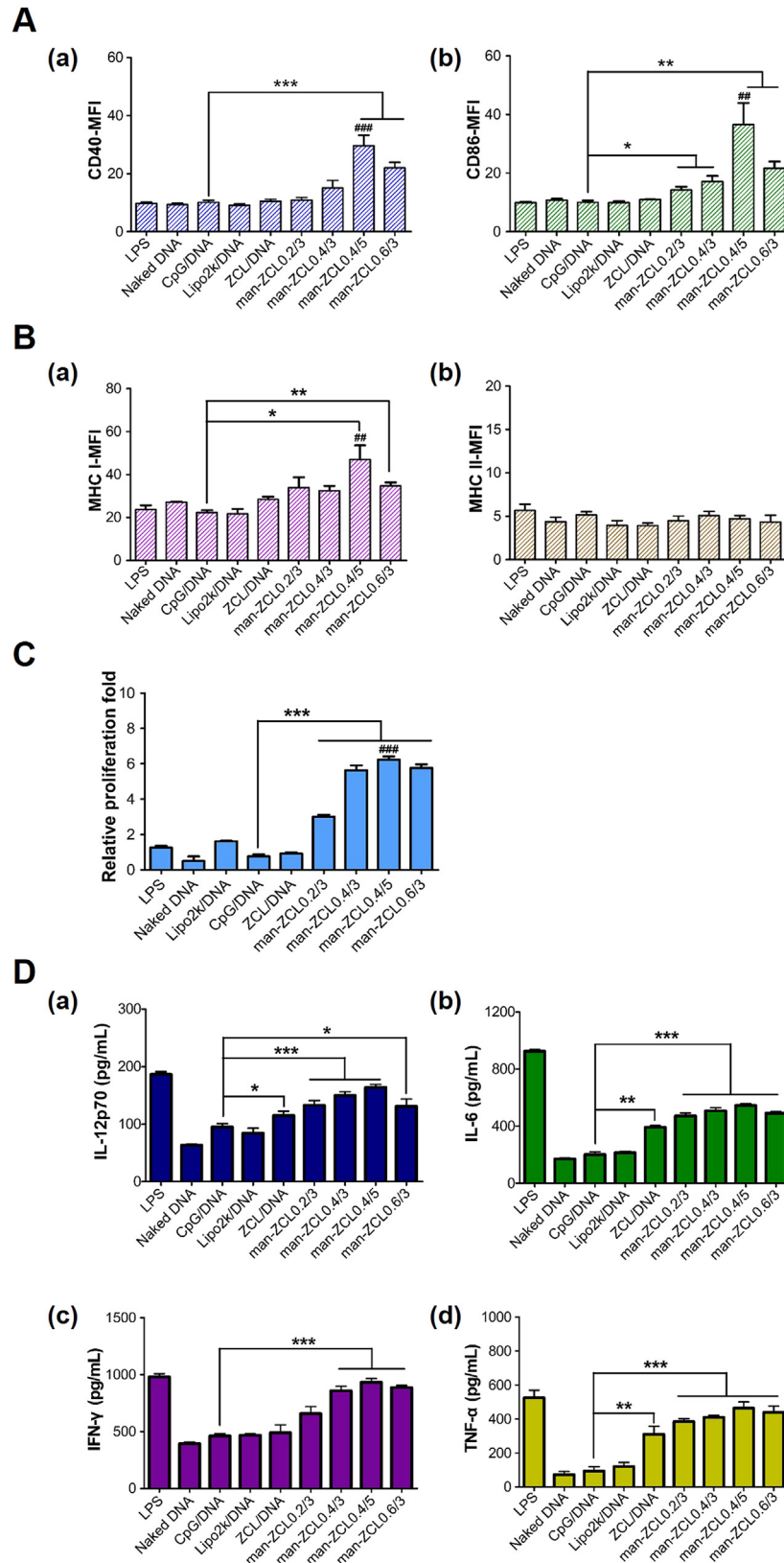
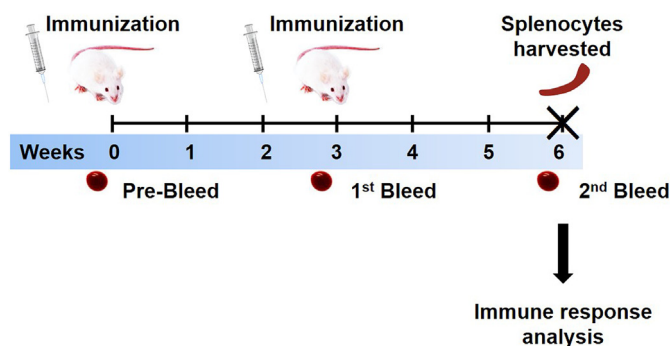


Fig. 7. Zwitterionic-based cationic lipoplexes promoted DC maturation. Immature DCs were incubated at 37 °C for 24 h with LPS, naked DNA, CpG/DNA, Lipo2k/DNA, ZCL/DNA (ZCL0.4/5), man-ZCL0.2/3, man-ZCL0.4/3, man-ZCL0.4/5 and man-ZCL0.6/3 formulations of cationic liposomes, respectively. Then the cells were labeled with anti-mouse monoclonal antibodies against the co-stimulators CD40, CD86 (A) or major histocompatibility complex class I, II (B) to detect their expression levels on the cell surface by flow cytometry. Zwitterionic-based cationic lipoplexes also induced the proliferation (C) and secretion of cytokines (IL12p70, IL-6, IFN- γ and TNF- α) (D) of DCs. Data shown as mean \pm SD, *: differences between CpG/DNA group with the group below the black line, *: $P < 0.05$, **: $P < 0.01$, ***: $P < 0.005$. #: differences between LPS group and man-ZCL0.4/5 group, ##: $P < 0.01$, ###: $P < 0.005$ (One-way ANOVA).



Scheme 2. Immunization schedule and detection program. Vaccine formulations were administered intramuscularly (i.m.) with an equivalent amount of 50 μ g DNA at week 0 and 3. Vaccine formulations divided equally between two hind quadriceps muscles. Serum was collected by retro-orbital puncture at week 0, 3 and 6 for the antibody detection and all mice were sacrificed 3 weeks after the last immunization and the spleen was removed, splenocytes were harvested for immunological assays.

important immune defense barriers to resist the invasion of HIV virus into organisms. After DNA antigen presentation, the protein-MHC complexes activated the naïve T cells and induced the immune responses. Herein, HIV-specific intracellular staining (ICS) was employed to examine the proportion of T cells (including CD3⁺, CD44⁺ and CD8⁺) and cytokines secreting CD3⁺ T cells (TNF- α and IFN- γ secreting CD3⁺ T cells) at the third week after last immunization (Scheme 2). The man-ZCL0.4/5 exhibited significant enhancement of Env-specific T cell proportion in comparison with CpG/DNA and ZCL/DNA (Fig. 8A, B). CD3⁺ T cells can transmit signals of T cell activation, which is of great importance in immune responses. And CD8⁺ T cells could eliminate the infected cells once the pathogen attacked again [6]. Moreover, the proportion of cytokines secreting Env-specific CD3⁺ T cells remarkably increased for the group vaccinated with man-ZCL0.4/5 (Fig. 8C). These results demonstrated that the Env-specific T cells could strongly activate and eliminate the infected cells when the mice were vaccinated with man-ZCL0.4/5 formulation.

To evaluate the bias of the immune response, the value of Th1/Th2 was illustrated (Fig. 8D) [36]. Th1 cells could secrete a variety of factors, such as interferon, which could promote CTL response, called the tendency of cellular immunity; while Th2 cells were associated with humoral immune responses to eliminate extracellular pathogens. In mice model, Th1 and Th2 cells induced the generation of IgG2a and IgG1, respectively, herein, the value of IgG2a/IgG1 was calculated to testify the Th1/Th2 ratio. As shown in Fig. 8D, all groups treated with man-ZCL lipoplexes exhibited a Th1/Th2 mixed immune responses ($1 < \text{Th1/Th2} < 2$), indicating that this DNA vaccines could elicit both cellular and humoral immunity. Since the groups treated with ZCL/DNA and man-ZCL/DNA lipoplexes exhibited enhanced cellular immunity responses as demonstrated in DCs maturation and HIV-specific responses *in vivo* (Fig. 7 and 8), they showed higher Th1/Th2 ratio compared with CpG/DNA lipoplexes group.

3.8. DNA vaccines retention at injection sites and accumulation in lymph nodes

The persistence at injection sites and accumulation in lymph nodes are important determinants of immunogenicity [37]. To evaluate DNA antigen persistence at the injection sites and accumulation in lymph nodes, fluorescence molecular Cy5-labeled HIV DNA plasmid Env (Cy5-DNA) was chosen as a model antigen. As shown in Fig. 9, the formulations with naked DNA or CpG/DNA resulted in rapid draining from the injection sites, and only 3% of

the original dose remained after 36 h post intramuscular administration (Fig. 9A, B). In contrast, administration of man-ZCL/DNA resulted in a significant high level of fluorescence intensity retention, which was higher than that of ZCL/DNA treated group (1.6-fold). The persistence time for ZCL/DNA and man-ZCL/DNA extended for 48 h and 60 h (the persistence time was calculated when about 20% of the original dose remained), respectively, which indicated that the man-ZCL/DNA system had a strong depot effect for longer release of the DNA antigens. The depot effect, which had been suggested to be primarily because of the electrostatic attraction between the cell membrane (negatively charged) and the cationic liposomes (positively charged), could provide a liposomal net to retain the antigen [38].

Immature DCs were draining to the lymph nodes during the maturation after capturing the antigens. Herein, the accumulation of DNA antigen in the nearby popliteal lymph nodes was also tested. As shown in Fig. 9C, man-ZCL0.4/5 exhibited a higher accumulation of DNA antigens in lymph nodes than that of other groups, which demonstrated that more DNA antigens were draining away and trafficking into lymph nodes with the aid of man-ZCL delivery systems. This suggested that man-ZCL0.4 was a potential DNA vaccine delivery system for enhanced immune responses.

3.9. Inflammatory responses at the injection sites

To investigate the *in vivo* toxicity of the man-ZCL lipoplexes, a histological analysis of muscles from the injection sites was performed (Fig. 10). Compared with the naked DNA group, groups treated with all man-ZCL/DNA lipoplexes showed a slight nuclear pyknosis and necrosis, while CpG/DNA group showed an obvious nuclear pyknosis and inflammatory cell infiltration. These results indicated that the group treated with CpG/DNA could induce strong inflammatory responses while groups treated with all man-ZCL/DNA lipoplexes could induce mild inflammatory responses. Throughout the whole vaccination period, the mice administrated with man-ZCL/DNA lipoplexes did not show any adverse effects. This histological analysis revealed that man-ZCL lipoplexes were safe for *in vivo* application.

3.10. Proposal process for man-ZCL as DNA vaccine adjuvant

The *in vitro* and *in vivo* results demonstrated that man-ZCL0.4/5 elicited enhanced immune responses and was a potential safe and effective DNA vaccine for the HIV DNA therapy. How did the man-ZCL lipoplexes undergo to trigger the strong immune response? Considering with the previous results, the suggested process was concluded and shown in Scheme 3. With the help of targeting molecules, the mannosylated ZCL lipoplexes were captured by the antigen processing cells (e.g. dendritic cells (DCs)) in the muscles. After entering the DCs via mannose-mediated endocytosis (1); the lipoplexes were internalized into endosomes/lysosomes, the zwitterionic lipid DSPE-PCB gradually changed from neutral to positive charge with the acidic proceeding, which led the fusion of zwitterionic-based cationic liposomes with the membranes of endosomes/lysosomes (2) and helped the DNA antigens escape to cytoplasm (3). This procedure was visible in the spinning disk confocal microscopy (Fig. 6 and Video S2). The endosomes/lysosomes were broken since the red fluorescence (lysosomes labeled by LysoTracker Red) was weakened or disappeared after separating with the green fluorescence (DNA labeled by YOYO-1). Then the released DNA entered into nuclei (4), and transcribed into HIV Env-specific antigen for presentation (5). Meanwhile, the zwitterionic-based cationic carriers might stimulate the APCs (4'), and help to activate the naïve T cell (5'). We found that the level of maturation of DCs was significantly increased when DCs were treated with the

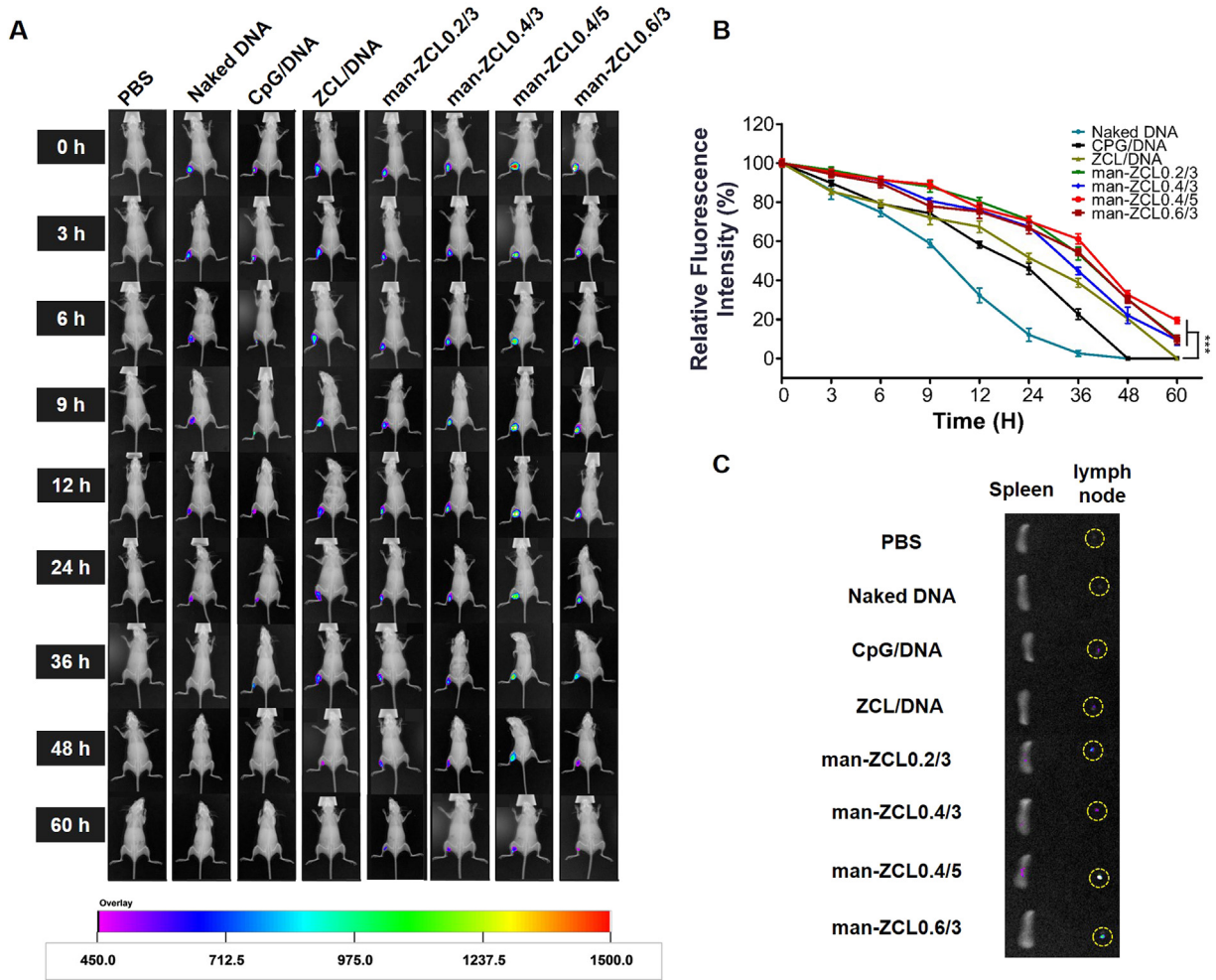


Fig. 9. Antigen retention at injection sites and accumulation in lymph nodes. (A) Representative fluorescence images and (B) quantitative fluorescence intensity of antigen retention at injection sites from 0.5 h to 60 h post injection; (C) Antigen transport into draining lymph nodes at 48 h after injection. BALB/c mice (n = 6) were intramuscularly injected with PBS, naked DNA, CpG/DNA, ZCL/DNA (ZCL0.4/5), man-ZCL0.2/3, man-ZCL0.4/3, man-ZCL0.4/5 and man-ZCL0.6/3 different DNA vaccine formulations containing Cy5-labeled HIV DNA plasmid Env, respectively. Data in (A) are representative for 6 results in each group. Data shown are mean ± SD, ***: P < 0.005.

man-ZCL lipoplexes, especially for man-ZCL0.4/5, but not for CpG/DNA or Lipo2k/DNA compared with naked DNA (Fig. 7). This

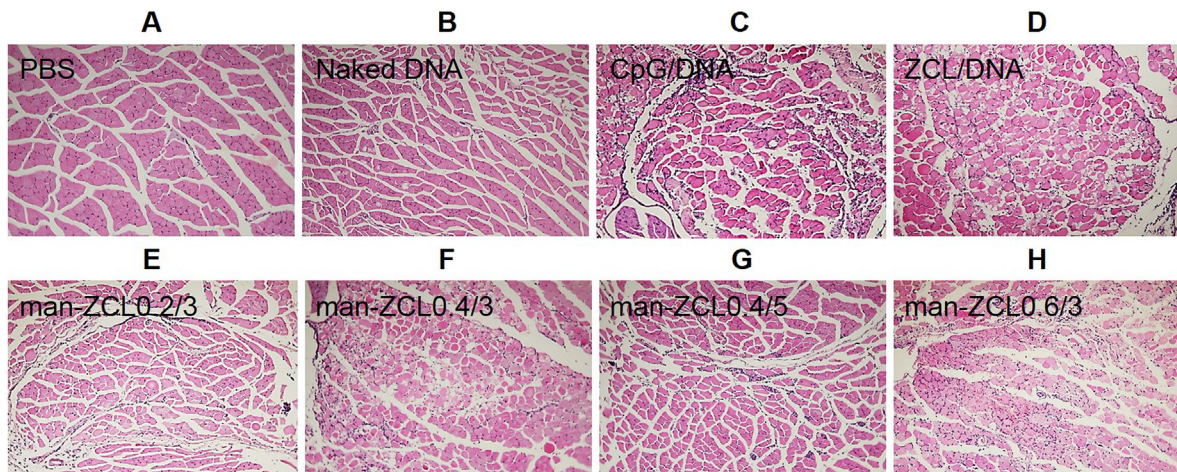
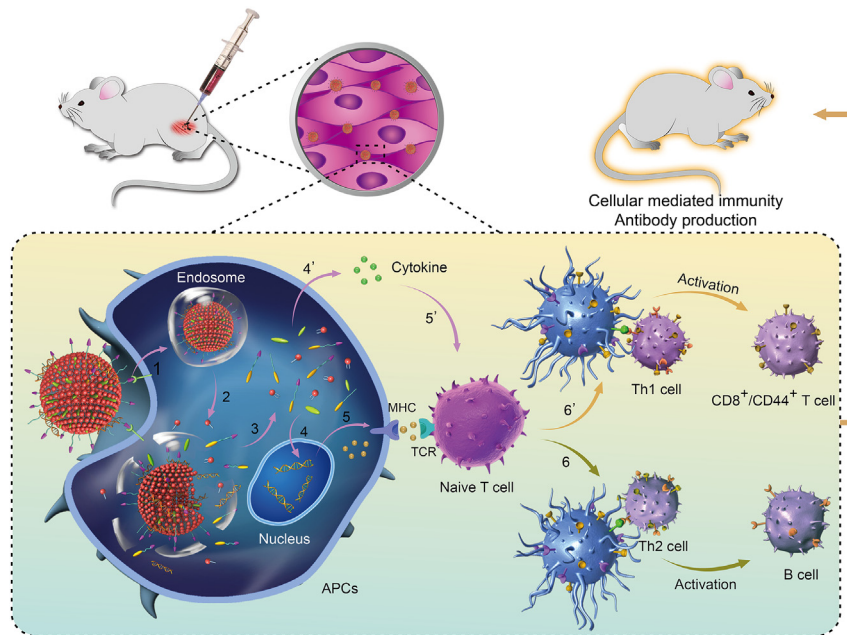


Fig. 10. Histological analysis of vaccine-associated inflammation at injection sites. BALB/c mice (n = 6) were intramuscularly injected with (A) PBS, (B) naked DNA, (C) CpG/DNA, (D) ZCL/DNA (ZCL0.4/5), (E) man-ZCL0.2/3, (F) man-ZCL0.4/3, (G) man-ZCL0.4/5 and (H) man-ZCL0.6/3 formulations vaccine formulations. Muscles from injection sites were isolated from mice at 48 h after immunization, embedded in paraffin, sectioned, and stained with hematoxylin and eosin to evaluate inflammation. 200× magnification.



Scheme 3. The mechanisms underlying the activation of APCs by man-ZCL/DNA lipoplexes. (1) endocytosis, (2) acidification and fusion with the membranes of endosomes/lysosomes (3) endosomes/lysosomes escape, (4) DNA enter into nuclei, (4') secret cytokines, (5) DNA antigen expression and presentation, activate the naïve T cells, (5') assistant to activate the naïve T cells, (6) activate the Th2 cells, (6') activate the Th1 cells.

indicated that man-ZCL lipoplexes could greatly promote DC maturation. And the concentration of zwitterionic lipid DSPE-PCB in liposomes and the N/P ratio in the lipoplexes had the important influence on the process of DC maturation. Compared with man-ZCLO.2, man-ZCLO.4 possessed more DSPE-PCB, which could help DNA antigen escape and enhance DNA presentation. As for man-ZCLO.6, the complex ability with DNA was larger than ZCLO.4 (Fig. 3C), and might limit the free release of DNA from the lipoplexes. As for man-ZCLO.4/3 and man-ZCLO.4/5, man-ZCLO.4/5 induced more cytokines for DC, which might be affected by the adjuvant of man-ZCL. This action was realized through a non-inflammasome pathway, and assisted to elicit strong immune responses (Fig. 7D).

After presenting to the naïve T cells, APC activated the Th1 and Th2 cells through major histocompatibility complex class I (MHC I) and class II (MHC II) molecules (6 and 6') and the cell-mediated immunity was significantly increased for man-ZCLO.4/5 delivery system, which was indicated by the level of MHC I molecules (Fig. 7B). This was due to the highest antigen presentation in DCs resulted by the enhanced cellular uptake and enhanced endosomal/lysosomal escape for man-ZCLO.4/5. For the *in vivo* vaccination, the present data suggested man-ZCL lipoplexes could activate Env-specific T cells greatly (Fig. 8), and trigger a Th1/Th2 mixed immune responses, which indicated that man-ZCL/DNA vaccines could elicit both cellular and humoral immune responses specifically for HIV DNA.

4. Conclusion

In conclusion, mannosylated zwitterionic-based cationic liposomes were constructed as a HIV DNA delivery carrier for *in vitro* and *in vivo* application. Our results demonstrated that the man-ZCL/DNA lipoplexes significantly enhanced the immunogenicity and anti-HIV immune responses in comparison with naked DNA, CpG/DNA and Lipo2k/DNA. This system greatly increased the cellular immunity and triggered a Th1/Th2 mixed immune responses. Moreover, the mannosylated zwitterionic-based cationic

lipoplexes as HIV DNA vaccines assisted activate T cells indirectly through a non-inflammasome pathway. This study indicates that the man-ZCL is a promising and potential adjuvant for DNA vaccines, and provides a safe and effective DNA vaccine strategy for HIV DNA clinical application in future.

Acknowledgments

This work was financially supported by the National Natural Science Foundation of China (21304099, 51573188, 31522023), the National High Technology Research and Development Program (2014AA020708) and the "Strategic Priority Research Program" of the Chinese Academy of Sciences (XDA09030301-3).

Appendix A. Supplementary data

Supplementary data related to this article can be found at <http://dx.doi.org/10.1016/j.biomaterials.2016.01.054>.

References

- [1] Y. Yang, W.L. Sun, J.J. Guo, G.Y. Zhao, S.H. Sun, H. Yu, et al., *In silico* design of a DNA-based HIV-1 multi-epitope vaccine for Chinese populations, *Hum. Vacc. Immunother.* 11 (2015) 795–805.
- [2] H. Kibuuka, R. Kimutai, L. Maboko, F. Sawe, M.S. Schunk, A. Kroidl, et al., A phase 1/2 study of a multiclade HIV-1 DNA plasmid prime and recombinant adenovirus serotype 5 boost vaccine in HIV-uninfected East Africans (RV 172), *J. Infect. Dis.* 201 (2010) 600–607.
- [3] X. Jin, C. Morgan, X.S. Yu, S. DeRosa, G.D. Tomaras, D.C. Montefiori, et al., Multiple factors affect immunogenicity of DNA plasmid HIV vaccines in human clinical trials, *Vaccine* 33 (2015) 2347–2353.
- [4] A. Endmann, K. Kluender, K. Kapp, O. Riede, D. Oswald, E.G. Talman, et al., Cationic lipid-formulated DNA vaccine against hepatitis B virus: immunogenicity of MIDGE-Th1 vectors encoding small and large surface antigen in comparison to a licensed protein vaccine, *Plos One* 9 (2014) 1–11.
- [5] D.N. Nguyen, J.J. Green, J.M. Chan, R. Longer, D.G. Anderson, Polymeric materials for gene delivery and DNA vaccination, *Adv. Mater* 21 (2009) 847–867.
- [6] L.G. Xu, Y. Liu, Z.Y. Chen, W. Li, Y. Liu, L.M. Wang, et al., Surface-engineered gold nanorods: promising DNA vaccine adjuvant for HIV-1 treatment, *Nano Lett.* 12 (2012) 2003–2012.
- [7] A. Li, L.L. Qin, W.R. Wang, R.R. Zhu, Y.C. Yu, H. Liu, et al., The use of layered double hydroxides as DNA vaccine delivery vector for enhancement of anti-

- melanoma immune response, *Biomaterials* 32 (2011) 469–477.
- [8] F.N. Al-Deen, J. Ho, C. Selomulya, C. Ma, R. Coppel, Superparamagnetic nanoparticles for effective delivery of malaria DNA vaccine, *Langmuir* 27 (2011) 3703–3712.
- [9] Y. Qiao, Y. Huang, C. Qiu, X.Y. Yue, L.D. Deng, Y.M. Wan, et al., The use of PEGylated poly [2-(N,N-dimethylamino) ethyl methacrylate] as a mucosal DNA delivery vector and the activation of innate immunity and improvement of HIV-1-specific immune responses, *Biomaterials* 31 (2010) 115–123.
- [10] E.V. Grant, M. Thomas, J. Fortune, A.M. Klibanov, N.L. Letvin, Enhancement of plasmid DNA immunogenicity with linear polyethylenimine, *Eur. J. Immunol.* 42 (2012) 2937–2948.
- [11] B. Ferraro, M.P. Morrow, N.A. Hutnick, T.H. Shin, C.E. Lucke, D.B. Weiner, Clinical applications of DNA vaccines: current progress, *Clin. Infect. Dis.* 53 (2011) 296–302.
- [12] K.K. Ewert, A. Zidovska, A. Ahmad, N.F. Bouxsein, H.M. Evans, C.S. McAllister, et al., Cationic liposome-nucleic acid complexes for gene delivery and silencing: pathways and mechanisms for plasmid DNA and siRNA, *Top. Curr. Chem.* 296 (2010) 191–226.
- [13] K.S. Korsholm, J. Hansen, K. Karlsen, J. Filskov, M. Mikkelsen, T. Lindstrom, et al., Induction of CD8+ T-cell responses against subunit antigens by the novel cationic liposomal CAF09 adjuvant, *Vaccine* 32 (2014) 3927–3935.
- [14] L.B. Dong, F. Liu, J. Fairman, D.K. Hong, D.B. Lewis, T. Monath, et al., Cationic liposome-DNA complexes (CLDC) adjuvant enhances the immunogenicity and cross-protective efficacy of a pre-pandemic influenza A H5N1 vaccine in mice, *Vaccine* 30 (2012) 254–264.
- [15] J. Liu, J.Q. Wu, B. Wang, S. Zeng, F.F. Qi, C.L. Lu, et al., Oral vaccination with a liposome-encapsulated influenza DNA vaccine protects mice against respiratory challenge infection, *J. Med. Virol.* 86 (2014) 886–894.
- [16] C.P. Locher, S.A. Witt, B.M. Ashlock, J.A. Levy, Evaluation of genetic immunization adjuvants to improve the effectiveness of a human immunodeficiency virus type 2 (HIV-2) envelope DNA vaccine, *DNA Cell Biol.* 23 (2004) 107–110.
- [17] Y. Li, Q. Cheng, Q. Jiang, Y.Y. Huang, H.M. Liu, Y.L. Zhao, et al., Enhanced endosomal/lysosomal escape by distearoyl phosphoethanolamine-polycarboxybetaine lipid for systemic delivery of siRNA, *J. Control. Release* 176 (2014) 104–114.
- [18] B. Carrillo-Conde, E.H. Song, A. Chavez-Santoscoy, Y. Phanse, A.E. Ramer-Tait, N.L.B. Pohl, et al., Mannose-functionalized “pathogen-like” polyanhydride nanoparticles target C-type lectin receptors on dendritic cells, *Mol. Pharm.* 8 (2011) 1877–1886.
- [19] J.S. Thomann, B. Heurtault, S. Weidner, M. Braye, J. Beyrath, S. Fournel, et al., Antitumor activity of liposomal ErbB2/HER2 epitope peptide-based vaccine constructs incorporating TLR agonists and mannose receptor targeting, *Biomaterials* 32 (2011) 4574–4583.
- [20] C.H. Jones, M.F. Chen, A. Ravikrishnan, R. Reddinger, G.J. Zhang, A.P. Hakansson, et al., Mannosylated poly(beta-amino esters) for targeted antigen presenting cell immune modulation, *Biomaterials* 37 (2015) 333–344.
- [21] R. Srinivas, A. Garu, G. Moku, S.B. Agawane, A. Chaudhuri, A long-lasting dendritic cell DNA vaccination system using lysinylated amphiphiles with mannose-mimicking head-groups, *Biomaterials* 33 (2012) 6220–6229.
- [22] C.H. Jones, M.F. Chen, A. Gollakota, A. Ravikrishnan, G.J. Zhang, S. Lin, et al., Structure function assessment of mannosylated poly(beta-amino esters) upon targeted antigen presenting cell gene delivery, *Biomacromolecules* 16 (2015) 1534–1541.
- [23] Y. Li, R.Y. Liu, Y.J. Shi, Z.Z. Zhang, X. Zhang, Zwitterionic Poly(carboxybetaine)-based cationic liposomes for effective delivery of small interfering RNA therapeutics without accelerated blood clearance phenomenon, *Theranostics* 5 (2015) 583–596.
- [24] J. Wang, R.R. Zhu, B. Gao, B. Wu, K. Li, X.Y. Sun, et al., The enhanced immune response of hepatitis B virus DNA vaccine using SiO₂@LDH nanoparticles as an adjuvant, *Biomaterials* 35 (2014) 466–478.
- [25] G.X. Ruan, Y.Z. Chen, X.L. Yao, A. Du, G.P. Tang, Y.Q. Shen, et al., Macrophage mannose receptor-specific gene delivery vehicle for macrophage engineering, *Acta Biomater.* 10 (2014) 1847–1855.
- [26] Z.P. Zhang, S. Tongchusak, Y. Mizukami, Y.J. Kang, T. Ioji, M. Touma, et al., Induction of anti-tumor cytotoxic T cell responses through PLGA-nanoparticle mediated antigen delivery, *Biomaterials* 32 (2011) 3666–3678.
- [27] Y.H. Jiang, M. Li, Z.R. Zhang, T. Gong, X. Sun, Enhancement of nasal HIV vaccination with adenoviral vector-based nanocomplexes using mucoadhesive and DC-targeting adjuvants, *Pharm. Res. Dordr.* 31 (2014) 2748–2761.
- [28] A.G. Kohli, P.H. Kierstead, V.J. Venditto, C.L. Walsh, F.C. Szoka, Designer lipids for drug delivery: from heads to tails, *J. Control. Release* 190 (2014) 274–287.
- [29] M.F. Bachmann, G.T. Jennings, Vaccine delivery: a matter of size, geometry, kinetics and molecular patterns, *Nat. Rev. Immunol.* 10 (2010) 787–796.
- [30] X.L. Bao, W. Wang, C. Wang, Y. Wang, J.P. Zhou, Y. Ding, et al., A chitosan-graft-PEI-candesartan conjugate for targeted co-delivery of drug and gene in anti-angiogenesis cancer therapy, *Biomaterials* 35 (2014) 8450–8466.
- [31] W.D. Zhang, Q. Cheng, S.T. Guo, D.S. Lin, P.S. Huang, J. Liu, et al., Gene transfection efficacy and biocompatibility of polycation/DNA complexes coated with enzyme degradable PEGylated hyaluronic acid, *Biomaterials* 34 (2013) 6495–6503.
- [32] Y.W. Noh, Y.S. Jang, K.J. Ahn, Y.T. Lim, B.H. Chung, Simultaneous in vivo tracking of dendritic cells and priming of an antigen-specific immune response, *Biomaterials* 32 (2011) 6254–6263.
- [33] Y.Q. Wang, J. Wu, Q.Z. Fan, M. Zhou, Z.G. Yue, G.H. Ma, et al., Novel vaccine delivery system induces robust humoral and cellular immune responses based on multiple mechanisms, *Adv. Healthc. Mater.* 3 (2014) 670–681.
- [34] K. Niikura, T. Matsunaga, T. Suzuki, S. Kobayashi, H. Yamaguchi, Y. Orba, et al., Gold nanoparticles as a vaccine platform: influence of size and shape on immunological responses in vitro and in vivo, *ACS Nano* 7 (2013) 3926–3938.
- [35] O. Lunov, T. Syrovets, C. Loos, G.U. Nienhaus, V. Mailander, K. Landfester, et al., Amino-functionalized polystyrene nanoparticles activate the NLRP3 inflammasome in human macrophages, *ACS Nano* 5 (2011) 9648–9657.
- [36] S.Y. Yan, B.E. Rolfe, B. Zhang, Y.H. Mohammed, W.Y. Gu, Z.P. Xu, Polarized immune responses modulated by layered double hydroxides nanoparticle conjugated with CpG, *Biomaterials* 35 (2014) 9508–9516.
- [37] D.S. Watson, A.N. Endsley, L. Huang, Design considerations for liposomal vaccines: influence of formulation parameters on antibody and cell-mediated immune responses to liposome associated antigens, *Vaccine* 30 (2012) 2256–2272.
- [38] M. Henriksen-Lacey, V.W. Bramwell, D. Christensen, E.M. Agger, P. Andersen, Y. Perrie, Liposomes based on dimethyldioctadecylammonium promote a depot effect and enhance immunogenicity of soluble antigen, *J. Control. Release* 142 (2010) 180–186.